University of Kent

Kent Academic Repository

Rodrigues, Caio Henrique Pinke, Mariotto, Lívia S., Mason, Nigel, Fantuzzi, Felipe and Bruni, Aline Thaís (2025) ***Towards analytical standards for new psychoactive substances: The contribution of computational chemistry and statistical methods.*** **Forensic Science International, 377 . ISSN 0379-0738.**

Downloaded from

https://kar.kent.ac.uk/115318/ The University of Kent's Academic Repository KAR

The version of record is available from

https://doi.org/10.1016/j.forsciint.2025.112642

This document version

Author's Accepted Manuscript

DOI for this version

Licence for this version

CC BY (Attribution)

Additional information

For the purpose of open access, the author(s) has applied a Creative Commons Attribution (CC BY) licence to any Author Accepted Manuscript version arising.

Versions of research works

Versions of Record

If this version is the version of record, it is the same as the published version available on the publisher's web site. Cite as the published version.

Author Accepted Manuscripts

If this document is identified as the Author Accepted Manuscript it is the version after peer review but before type setting, copy editing or publisher branding. Cite as Surname, Initial. (Year) 'Title of article'. To be published in ***Title of Journal*** , Volume and issue numbers [peer-reviewed accepted version]. Available at: DOI or URL (Accessed: date).

Enquiries

If you have questions about this document contact ResearchSupport@kent.ac.uk. Please include the URL of the record in KAR. If you believe that your, or a third party's rights have been compromised through this document please see our Take Down policy (available from https://www.kent.ac.uk/guides/kar-the-kent-academic-repository#policies).

Towards Analytical Standards for New Psychoactive Substances: The Contribution of Computational Chemistry and Statistical Methods

Caio Henrique Pinke Rodrigues,[a,b] Lívia Salviano Mariotto,[a,c] Nigel J. Mason,[d] Felipe Fantuzzi,[c] and Aline Thais Bruni[a,b,e]*

[a] Department of Chemistry, Faculty of Philosophy, Sciences and Letters of Ribeirão Preto, Ribeirão Preto, São Paulo 14040-091, Brazil
[b] Instituto Nacional de Ciência e Tecnologia – Ciências Forenses (INCT Forense), Department of Chemistry, Faculty of Philosophy, Sciences and Letters of Ribeirão Preto, Ribeirão Preto, São Paulo 14040-091, Brazil
[c] School of Chemistry and Forensic Science, University of Kent, Park Wood Rd, Canterbury CT2 7NH, UK
[d] School of Physics and Astronomy, University of Kent, Park Wood Rd, Canterbury CT2 7NH, UK
[e] Instituto Nacional de Ciência e Tecnologia – Ciências Forenses (INCT SP), Department of Chemistry, Faculty of Philosophy, Sciences and Letters of Ribeirão Preto, Ribeirão Preto, São Paulo 14040-091, Brazil

* corresponding author's email: aline.bruni@usp.br

ORCID

Caio Henrique Pinke Rodrigues: 0000-0002-7794-7484
Lívia Salviano Mariotto: 0000-0002-8536-0990
Nigel J. Mason: 0000-0002-4468-8324
Felipe Fantuzzi: 0000-0002-8200-8262
Aline Thais Bruni: 0000-0002-7721-3042

- Computational IR spectroscopy can help in NPS characterization.
- Statistical models validate theoretical and experimental spectral alignment.
- SWOT analysis shows advantages and limitations of computational tools.
- Machine learning and AI enhance spectral prediction for emerging NPS.

Manuscript (without author details)

Click here to view linked References

Towards Analytical Standards for New Psychoactive Substances: The Contribution of Computational Chemistry and Statistical Methods

Abstract

New psychoactive substances (NPS) present significant challenges for law enforcement and public health due to their rapid emergence and structural diversity, often outpacing the development of traditional analytical methods. This review explores using computational chemistry, particularly density functional theory (DFT), to obtain infrared spectra. This combination to characterize NPS began in the 2010s and has gained momentum across all continents in recent years. In the review, we demonstrate that DFT can accurately predict the spectroscopic properties of NPS. In addition, statistical methods for comparing computational and experimental data were presented. A SWOT (Strengths, Weaknesses, Opportunities, Threats) assessment was performed to assess the potential and limitations of these computational approaches. Finally, integrating artificial intelligence and developing extensive spectral databases emerge as promising avenues for future research, provided that data reliability and rigorous validation processes are maintained. All these efforts are aligned to obtain faster responses and keep up with NPS advances.

Keywords: New Psychoactive Substances, Quantum Chemistry, Density Functional Theory, SWOT

1. Introduction

New Psychoactive Substances (NPS) represent a diverse group of compounds not regulated by the Single Convention on Narcotic Drugs (1961) or the 1971 Convention on Psychotropic Substances. The term "new" does not necessarily mean recently synthesized but refers to substances that have gained attention due to their significant potential for abuse and public health risks. Their structural diversity and rapid emergence highlight the urgent need for efficient and non-destructive analytical techniques to support decision-making related to these compounds [1–4].

Fundamentally, spectroscopic techniques rely on the interaction of matter with radiant energy, which involves transmission, absorption, or reflection. Spectroscopic methods have demonstrated their effectiveness in providing the necessary insights to address this evolving issue [5]. In the forensic domain, the SWGDRUG classifies IR spectroscopy as a "Category A" technique, the highest classification for its selectivity and ability to provide structural information [6]. Among these techniques, near- and mid-infrared (NIR and MIR) spectroscopies stand out for their accessible implementation and rapid response time [7–11]. More specifically, they offer quick acquisition of results, non-destructive sample analysis, low-cost instrumentation, and minimal sample preparation. Moreover, they are versatile, applicable to liquid, semi-solid, and solid samples [12,13].

To complement spectroscopic methods, computational approaches have become essential in the characterization of NPS. Experimental methods for spectroscopy of these substances often require expensive and time-consuming techniques, while the rapid availability of information is essential to reduce uncertainties about their behavior [14]. Recognizing the limitations in drug detection also paves the way for the development of alternative methodologies capable of addressing the challenges posed by NPS [15]. Computational methods predict spectral properties without requiring physical samples or laboratory resources, making them sustainable and cost-effective alternatives. By eliminating the need for reference standards, computational tools enable systematic studies of emerging compounds and provide reliable data for substances with limited prior characterization [16]. In the case of NPS, too many structural similarities can compromise assertive identification [17–19].

This study aims to evaluate the role of computational approaches in the characterization of NPS through infrared spectroscopy. Understanding these substances can enhance decision-making and address challenges related to NPS.

2. Short Background

In chemistry history, many theories and methods have been proposed, but in the last century, an approach that has shown effective for quantum chemical calculations was Density Functional Theory (DFT) [20–24]. Building upon the foundational work of Hohenberg and Kohn (1964) [25] and the practical framework introduced by Kohn and Sham (1965) [26], DFT reformulates the many-electron problem in terms of the electron density rather than the many-body wavefunction [27–29].

In quantum mechanics, the energy levels associated with particle motion are *quantized* in bound systems, meaning particles can only occupy discrete energy levels for translational, rotational, and vibrational motions. Electrons can also undergo transitions between quantized electronic energy levels [30]. Specifically, DFT expresses the total electronic energy as a function of the electron density, which is composed of different components: the kinetic energy, the electron-nucleus attraction energy, the classical Coulomb electron-electron repulsion energy, and the exchange-correlation energy functional (E_{xc}).[27,31]. E_{xc} arises from quantum mechanical effects, including exchange effects, originating due to the antisymmetry of the electronic wavefunction, reflecting the Pauli exclusion principle; and correlation effects, arising from the dynamic correlation of electron motions that are not captured by the mean-field approximation [11,27,32–34]:

Pure DFT methods utilize various exchange-correlation functionals to approximate the exchange and correlation energies of a system. For instance, the BLYP functional combines Becke's exchange functional [35] with the Lee-Yang-Parr correlation functional (LYP) [36], which is derived from the Colle-Salvetti correlation energy formula and depends on the electron density and its gradient [37]. Hybrid methods, such as B3LYP (Becke, three-parameter, Lee-Yang-Parr), are frequently used in organic molecule analysis. B3LYP incorporates a mixture of exact Hartree-Fock exchange with DFT exchange-correlation functionals, with parameters determined empirically [11,27,29]. These methods yield discrete values for energy and structural parameters (bond lengths and angles). In quantum chemical calculations, including DFT, basis sets are used to represent atomic orbitals and electron distributions, and the choice of basis set is crucial for accurately describing the valence shell and obtaining reliable results.

The mathematical representation of the valence shell is an essential factor for achieving convergence and accurate results in quantum chemical calculations. Basis sets are collections of functions used to describe the atomic orbitals in molecules [38,39]. One widely used family of basis sets is the Pople basis sets, developed by John Pople and co-workers. These basis sets distinguish between core (inner-shell) and valence electrons by employing split-valence

orbitals. The 3-21G basis set is one of the simplest in this family and serves as a starting point for many calculations. In the 3-21G basis set, the core orbitals are represented by a single contracted Gaussian function composed of three primitive Gaussian functions. The valence orbitals are split into two parts: one represented by a contraction of two primitive Gaussian functions and another by a single primitive Gaussian function [40].

Building upon this, the 6-31G basis set provides a more flexible and accurate description [41]. These split-valence basis sets allow for a better representation of valence electron distributions, which is essential for accurately modeling chemical bonding and reactions [42]. For atoms in the second and third periods of the periodic table, adding d-type polarization functions improves the description of molecular properties [28,29]. For hydrogen and other atoms where s-functions are the valence functions, adding p-type polarization functions can be beneficial. The addition of polarization functions is indicated in the basis set notation [43,44].

It is important to note that Pople-type basis sets [44] are just one option among many. Other basis sets, each designed with different corrections, approximations, and representations, are also commonly used. For example, the Sadlej sets (e.g., DZP, TZ2P, Sadlej-pVTZ) are optimized for accurate calculations of electric properties, such as dipole moments and polarizabilities [45]. Dunning's correlation-consistent basis sets, known as cc-pV*Z (where * represents the cardinal number D, T, Q, etc., for double, triple, quadruple zeta), such as cc-pVDZ and cc-pVTZ, are designed for systematic convergence in correlated calculations [46]. Effective Core Potential (ECP) basis sets, including LANL2DZ[47,48] and SDD [49], replace the inner core electrons of heavy atoms with a potential, reducing computational cost while effectively modeling core-valence electron interactions. The Ahlrichs basis sets include SVP and TZVP [50]; their improved versions, the def2 basis sets (e.g., def2-SVP, def2-TZVP, def2-TZVPP), offer enhanced accuracy and efficiency [51]. These diverse basis sets provide a range of options for performing detailed spectroscopic and electronic structure analyses, aiding in the characterization and differentiation of a wide variety of molecules.

Spectroscopic responses can be obtained using these sets of functionals and bases, as this response shows the interaction between matter and electromagnetic radiation as a function of the radiation’s wavelength or frequency. It examines the absorption, emission, or scattering of energy by atoms and molecules [10]. Spectroscopy provides graphical representations, known as spectra, which depict the amount of energy absorbed or emitted by molecules and atoms at different wavelengths or frequencies [52]. The theoretical spectra show the harmonic oscillator approximation, where chemical bonds are modeled as idealized springs exhibiting simple harmonic motion. Nevertheless, real molecular vibrations deviate from this simplified model due to anharmonicity—the potential energy surface of a real molecule is not perfectly parabolic,

especially at higher vibrational energies where bond stretching can lead to bond breaking [34,53,54].

In addition, computational methods often require experimental reference data to accurately align theoretical predictions with observed infrared spectra. Through the integration of theoretical calculations and experimental data, it is possible to obtain key information about chemical structures, enabling more accurate spectroscopic characterization [55]. This synergetic, integrated approach has found extensive applications in fields such as materials science, molecular design, and structural analysis, where precise understanding and prediction of molecular behavior are critical.

3. DFT Applications

Density functional theory (DFT) has widespread applications across various fields, driven by advancements in computational power and improved correlations between theoretical and experimental results. These developments have enabled the exploration of new areas such as metalloproteins [56], electrocatalysis [57], bioelectrochemistry [58], batteries [59], diseases [60], and many others [32,61–63]. In addition to these applications, the forensic field has greatly benefited from DFT, particularly in the identification and characterization of drugs of abuse.

Quantum chemistry calculations, such as those using DFT, are valuable tools for obtaining spectroscopic information, including vibrational frequencies corresponding to the fundamental vibration modes of molecules. These computationally derived frequencies can be directly correlated with vibrations observed in the NIR (near infrared) and MIR (mid infrared) regions of the spectrum. While some studies have extended these analyses to FIR [53,55], research in this area remains relatively scarce compared to the more extensively studied NIR and MIR regions. Comparisons between theoretical and experimental spectra allow for the assignment of specific absorption bands to discrete energy values associated with computationally obtained vibrations. This process involves analyzing the relative intensities and positions of peaks in the spectra, enabling the validation of theoretical models and refining the understanding of the molecular vibrations [55,64,65].

This combination of theoretical and experimental approaches facilitates the accurate differentiation of structurally similar molecules—those with closely related chemical structures or functional groups [55]. This is particularly valuable in cases where experimental techniques alone may struggle to distinguish between such molecules, as exemplified by fentanyl analogs [66], synthetic cannabinoids [67], and cathinones [68]. Ensuring optimal alignment between simulated and experimental data depends critically on the choice of the appropriate DFT

functional. For example, Dogruer Erkok et al. (2024) [66] advise against using B3LYP without dispersion corrections for fentanyl analogs, recommending instead the ωB97X-D functional [69] as a better choice. In the case of fluorinated molecules, Kreienborg and Merten (2019) [70] highlight the superior performance of the M06-2X functional [71] over B3LYP for these systems [72]. Similarly, Džodić et al. (2024) [73] demonstrated that the M05-2X functional [74], an earlier generation Minnesota-type functional related to M06-2X, outperformed B3LYP in describing benzodiazepines and their common adulterants or diluents.

Figure 1 summarizes the results of a bibliographic search for studies employing computational methods to simulate the infrared spectra of psychoactive substances. It provides details on the year of publication, the country of the corresponding author's institution, the DFT functionals and basis sets utilized, the application of Grimme's empirical dispersion corrections [75–77], the computational software and its version, and the class of substances investigated.

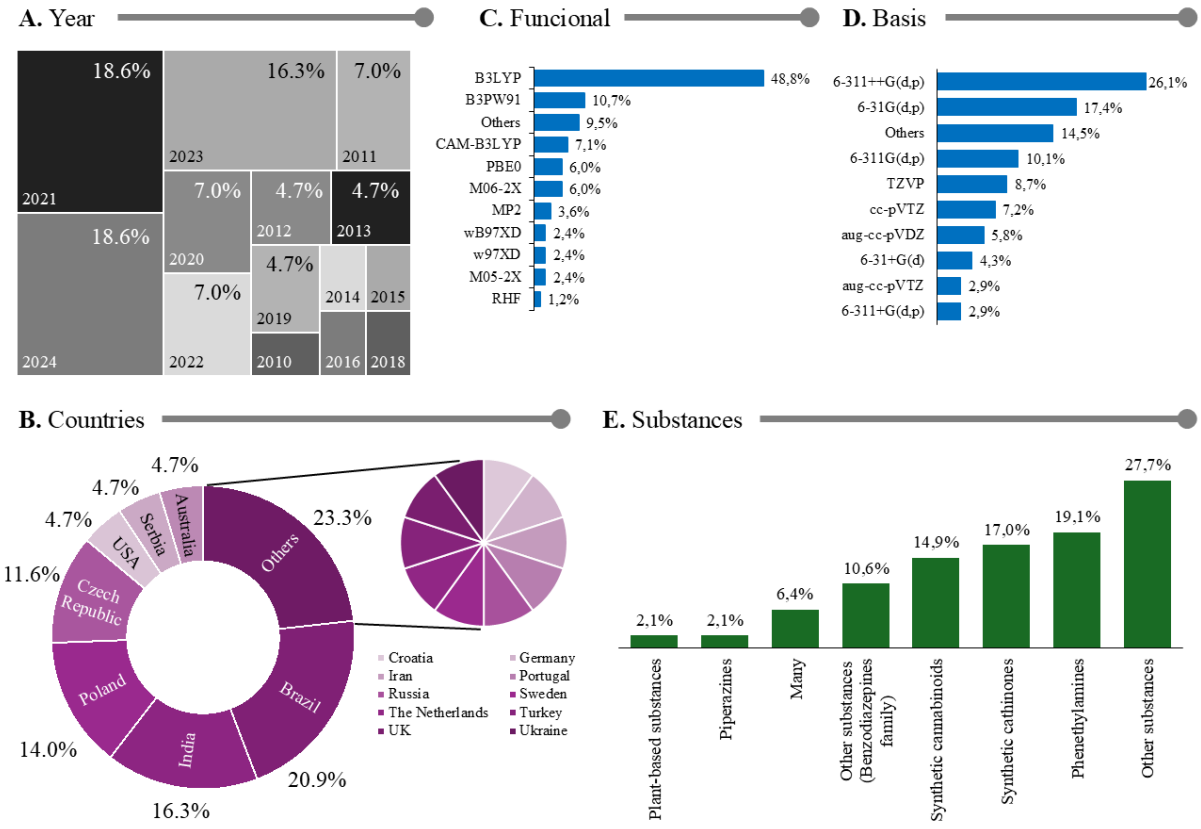

Figure 1. Information present in the evaluated articles on the use of DFT to obtain spectra in the infrared region for NPS being (A) the years in which the works were published and the respective percentage of the total (43); (B) the countries of the corresponding authors; (C) the main functionals used in the analyzed works and (D) the respective bases; and (E) the classes of substances studied in the selected articles.

The first studies using theoretical chemistry to simulate the infrared spectra of NPS emerged in the early 2010s, around the same time as the first reports of seizures of these

substances. Since then, the application of these methods has expanded across various studies and substance types, with researchers conducting studies on nearly every continent. Based on the information in **Figure 1**, the most used combination of DFT functional and basis set is B3LYP (48.8%) with a Pople-type basis (specifically 6-311++G(d,p) with 26.1%). This combination is particularly effective for organic structures due to the intrinsic parameters of the functional.

The countries that stand out with the highest number of publications on the subject were Brazil (20.9%), India (16.3%) and Poland (14.0%). However, other countries stand out and have publications with more significant impact. When we evaluate the substances studied and according to the UNODC classification, the main ones were phenylethylamines (19.1%), cathinones (17.0%), and synthetic cannabinoids (14.9%). Additionally, the commercial software Gaussian (in various versions) is the most widely used tool, largely due to its user-friendly graphical interface. However, studies using free software Orca — although lacking a graphical interface — have shown comparable performance to Gaussian.

3.1. Conformational Analysis

In addition to selecting an appropriate computational method, conformational analysis is one of the most critical steps to ensure accurate computational results. Since the chemical properties of a molecule are intrinsically tied to its three-dimensional arrangement—and this arrangement determines the electronic properties of the compound—conformational analysis is a fundamental starting point for any theoretical chemistry study of a drug [78,79].

This procedure aims to explore the potential spatial arrangements of a molecule, including bond lengths, bond angles, and dihedral angles, to identify the most stable structure based on its energy. By systematically stretching and twisting a molecule and plotting a graph of its energy as a function of these changes, a potential energy surface (PES) is generated. The PES graph reveals regions of maximum energy, representing unfavorable atomic arrangements, and regions of minimum energy, corresponding to stable configurations. These minima can be either local or global, with transition regions between maxima and minima representing intermediate states [80–82]

Several methods are available for conducting conformational analysis, which will be detailed below. However, it is crucial to emphasize that all such procedures must be carried out systematically and carefully. The three-dimensional structure directly influences spectroscopic responses; any oversight in this process could lead to significant errors. These may include incorrect mode assignments or observer bias when comparing spectral bands [83].

The Systematic Search method aims to explore possible conformations of chemical structures by applying discrete variations to dihedral angles—the angles formed by four bonded atoms—using predetermined values. Once these conformations are optimized using a combination of DFT functional and basis set, parameters such as Gibbs free energy can be obtained alongside various physicochemical and structural data [78,80,84]. For instance, Baranska et al. (2012) [85] applied this approach to determine the minimum energy structures of nicotine on the PES. By incrementally rotating the free bond in the molecule by 15°, they identified two stable conformations corresponding to the *cis* and *trans* arrangements of nicotine. Similarly, Dobšíková et al. (2023) [72] used a systematic search to study the structures of two cathinone hydrochlorides—(*S*)-2-(methylamino)-1-(3-(trifluoromethyl)phenyl)propan-1-one and (*S*)-2-(methylamino)-1-(3-(trifluoromethyl)phenyl)pentan-1-one—to enable enantiomeric separation of the conformers.

Andernach et al. (2016) employed this approach to determine the absolute configuration of the synthetic cannabinoid MDMB-CHIMICA, which had not been experimentally characterized at the time [86]. Similarly, Spálovská et al. (2019) analyzed the structures of two cathinones—methylone and pentylone—and identified the existence of multiple stable conformers in aqueous solution. This insight aids in understanding spectrophotometric responses, which depend on the three-dimensional structure of molecules [87]. Additional studies have applied these methodologies to other substances, such as amphetamine-type stimulants [83], phenylethylamines [88], and natural products [81].

3.2.Building of theoretical spectra

Unlike experimental spectra, which may be obtained in solution or in the solid state, computational calculations often assume isolated molecules in a vacuum. This method of generating spectra results in specific combinations of wavelength and signal intensity, producing a fine spectral line profile. In experimental spectra, broader areas under the curve are typically observed due to effects not accounted for in simulations, such as the Doppler effect, particle collisions (both among particles and between particles and the medium), and proximity broadening. Additionally, factors such as temperature, pressure, concentration, and phase can influence the spectra [10,89]. Consequently, even with high-resolution instrumentation, experimental spectra often exhibit broader spectral bands or lines. To make simulated spectra resemble experimental profiles, mathematical treatments are required.

The spectral line profile describes the shape of the electromagnetic spectrum, in this case, in the infrared region, through areas of varying intensity [90]. Several functions can be used to

model this profile, such as the Lorentz function (or Cauchy distribution), Gaussian function, and Voigt function. These functions rely on parameters such as full width at half maximum (FWHM), line position, and maximum peak height. Due to their mathematical properties, these functions are symmetrical around the reference peak [91,92]. However, for forensic purposes, only the Lorentzian and Gaussian functions are commonly employed, represented by **Equations 1** and **2**, respectively:

$$L = \frac{1}{1 + x^2} \quad \textbf{(1)}$$

$$G = e^{-(ln2).x^2} \quad \textbf{(2)}$$

The term x in these equations is defined as:

$$x = \frac{(p - p_0)}{w/2} \quad \textbf{(3)}$$

Where L is the Lorentzian function, G is the Gaussian function, p is the peak position in the spectrum, p_0 is the maximum value in the spectrum, and w is the FWHM (full width at half maximum). The normalization due to x ensures a maximum value of 1 at $x = 0$ and a value of 1/2 at x ±1. [90–92]. The FWHM parameter w can vary depending on the study: examples include 6 cm^{-1} [86], 8 cm^{-1} [83,93], 10 cm^{-1} [72,87,94], 24 cm^{-1} [95], and 45 cm^{-1} [64].

Several studies have used the Lorentzian function to model infrared spectra. These include work on amphetamine and methamphetamine [66,72,83,93–95], cathinones [72,93], fentanyl analogs [66,94], and other substances [95].

Similarly, the Gaussian function has been applied in studies of amphetamine and cathinone analogs [19,64,68,96], phenylethylamine derivatives (2C, NBOH, and NBOMe) [88] , fentanyl analogs [97], drug metabolites [64], and various other substances [98]

In addition to these methods, alternative software and algorithms have been explored. MultiWFN [99] employs Lorentzian functions as its foundation, while SpecDis [100] incorporates various features. For instance, Wang et al. (2019) [101] used MultiWFN to generate spectra for fentanyl and six structural analogs. Similarly, Andernach et al. (2016) [86] utilized SpecDis to obtain the spectrum of the absolute configuration of the synthetic cannabinoid MDMB-CHIMICA.

3.2.1. Scaling Factors

From an experimental perspective, certain phenomena, such as perturbations, oscillations, and interactions, are observed in IR spectra. Simulated spectra, on the other hand, primarily

represent harmonic vibrational oscillations calculated using numerical integration techniques. The discrepancies between experimental and theoretical spectra arise due to anharmonic effects, basis set incompleteness, the neglect of Morse potential effects for bonds, and electronic correlation limitations [94,95]. While simulations that account for these effects are possible, they often come with significant computational costs [11,29]. These scaling factors correct systematic errors arising from the harmonic approximation and the specific combination of DFT functional and basis sets used in the calculations [102]. They are empirically derived by comparing calculated frequencies to experimental data and are specific to each computational method [8,10,103].

Specific vibrational modes or regions of interest in the spectrum are often used to derive correction factors to address deviations between theoretical and experimental vibrational frequencies [11,29,104]. These correction factors are typically calculated as the ratio of the experimental vibrational frequency (ν_{exp}) to the theoretical vibrational frequency (ω_{cal}), expressed as $\lambda = \nu_{exp}/\omega_{cal}$, where λ represents the dimensionless correction factor [101]. A commonly used reference vibration is the C=O stretching mode, typically occurring at 1625 cm^{-1} [10,105]. Alternatively, correction factors can be applied to different frequency regions of the IR spectrum, enabling the use of multiple correction factors within a single computationally derived spectrum [101].

Table 1 presents the scaling factors reported in the literature for correcting IR spectra of psychoactive substances, summarizing the associated DFT functionals and basis sets used in each case. These scaling factors are applied to align computationally derived vibrational frequencies with experimental results, and their values are generally close to unity, reflecting substantial agreement between theoretical predictions and experimental outcomes. Specifically, the mean, median, and mode of the correction factors were 0.9660, 0.9670, and 0.9800, respectively, with a standard deviation of ±0.0290 [106]. These results emphasize that each DFT functional and basis set pair requires specific adjustments, although the observed deviations are minor.

Table 1. Scaling factors used for each set of DFT functionals and as a basis for works involving the simulation of psychoactive substances.

Method[a]	Basis set	Scaling factor	Reference
A specific correction factor—a single DFT functional and basis set—applied to the entire spectrum.			
HF	6-31G(d,p)	0.902	[107]
B3LYP	6-311G(d)	0.965	[53]
B3LYP	6-31G(d,p)	0.960	[107]
B3LYP	6-311G(d)	0.955	[55]
B3LYP	6-31+G(d,p)	0.9642	[108]
B3LYP	6-311++G(d,p)	0.9800	[109]
B3LYP	6-311++G(d,p)	0.961	[110]
B3LYP	6-31G(d,p)	0.9608	[17]

B3LYP	aug-cc-pVDZ	0.9824	[85]
B3LYP	TZVP	0.9654	[17]
B3LYP	TZVP	0.9650	[68]
B3LYP	6-311++G(d,p)	0.945	[111]
B3LYP	TZVP	0.9654	[98]
B3LYP	def2-TZVP	1.0044	[88]
PBE	TZVP	1.0306	[67]
PBE0	6-31G(d,p)	0.9863	[17]
PBE0	def2-TZVP	0.9944	[88]
PBE0	TZVP	0.9888	[17]
PBE0	TZVP	0.9596	[98]
ωB97X-D	cc-pVTZ	0.9660	[66]
M06-2X	TZVP	0.9462	[98]
B3PW91	TZVP	0.9643	[98]
Perdew–Zunger	Normconserving pseudopotentials	0.9700	[94]
A specific correction factor—a single DFT functional and basis set—applied to different regions of the spectrum.			
HF	6-311+G(d,p)	0.8451 (< 1000 cm^{-1}) 0.9101 (> 1000 cm^{-1})	[112]
B3LYP	6-311+G(d,p)	0.9401 (< 1000 cm^{-1}) 0.9610 (> 1000 cm^{-1})	[112]
B3LYP	6-311G(d,p)	0.98707 (< 1800cm^{-1}) e 0.94993 (2800–3200 cm^{-1})	[113]
B3LYP	6-311++G(d,p)	0.950 (high frequency region with CH stretching modes) 0.978 (rest of the spectrum)	[93]
Non-specific correction factors or those applicable to multiple DFT functional/basis set combinations—applied to the entire spectrum.			
B3LYP	6-31G(d), 6-311G(d,p)	0.984	[86]
B3LYP	6-31G(d), 6-31+G(d,p), 6-31++G(d,p), 6-311++G(d,p)	0.971	[95]
B3LYP	6-31G(d), 6-311G++(d,p)	0.980	[114]
B3LYP	6-311+G(d,p), LANL2DZ for iodine	0.967	[115]
B3LYP	6-311+G(2d,p), cc-pVTZ	0.9679	[116]
B3LYP, HSEH1PBE	6-311++G(d,p)	0.9615	[117]
B3LYP, B3LYP-D3, M06-2X	6-31G(d,p)	0.961	[19]
B3LYP, MP2	6-311++G(d,p)	0.967	[118]
B3LYP, CAM-B3LYP	6-311++G(d,p)	0.978	[119]
B3LYP, B3LYP-D3BJ, B3PW91, CAM-B3LYP, M05-2X, M06-2X	6-311++G(d,p)	0.910	[73]
B3LYP, MP2	6-311+G(d,p)	0.975	[64]
B3LYP, CAM-B3LYP, B3PW91, M06-2X, M05-2X	6-311++G(d,p)	0.930	[105]
B3LYP, B3PW91, CAM-B3LYP, ωB97X-D, M06-2X	6-311++G(d,p), aug-cc-pVDZ, aug-cc-pVTZ	0.9800	[72]
B3LYP, ωB97X-D	6-311G(d,p), cc-pVTZ	0.9660	[101]
B3LYP, B3PW91, CAM-B3LYP	6-311++G(d,p), aug-cc-pVDZ, aug-cc-pVTZ	0.9800, 0.9900, 0.9900	[120]
B3LYP, PBE0	TZVP, 6-311G(d,p)	0.9670	[97]
MP2, B3LYP, X3LYP, B3PW91	6-31+G(d), 6-311++G(d,p), 6-311++G(2d,2p), cc-pVDZ, cc-pVTZ	0.9750	[121]
B3LYP, B3PW91	6-31G(d), 6-311++G(d,p)	0.9900 and 0.9800	[87]
B3LYP, B3PW91	6-31G(d), 6-311++G(d,p)	derived from the same paper	[83]

[a] Besides DFT, some authors also utilize wavefunction-based calculations, including Hartree–Fock (HF) and post-HF methods, such as second-order Møller–Plesset perturbation theory (MP2).

The Computational Chemistry Comparison and Benchmark Database (CCCBDB), maintained by the National Institute of Standards and Technology (NIST), provides a valuable resource for researchers seeking correction factors. This database offers standardized data for various DFT functional and basis set combinations, widely used by research groups to align computational predictions with experimental results [122]. Despite its utility, some studies in the literature, as highlighted in **Table 1**, fail to specify whether correction factors were explicitly applied to individual cases or uniformly across all methods. These omissions underscore the importance of clarity and standardization in reporting computational procedures.

Providing a benchmark for such efforts, Irikura et al. (2005) [123] conducted a comprehensive analysis of the uncertainties associated with correction factors arising from the choice of DFT functional and basis set. Their analysis included a graphical representation of the frequency distribution of these correction factors, as shown in **Figure 2**. Notably, the most frequent values, comprising 45.3% of the data (31 of 53), fell within the range of 0.9531–0.9801, further supporting the strong consistency between theoretical data and experimental spectroscopic results.

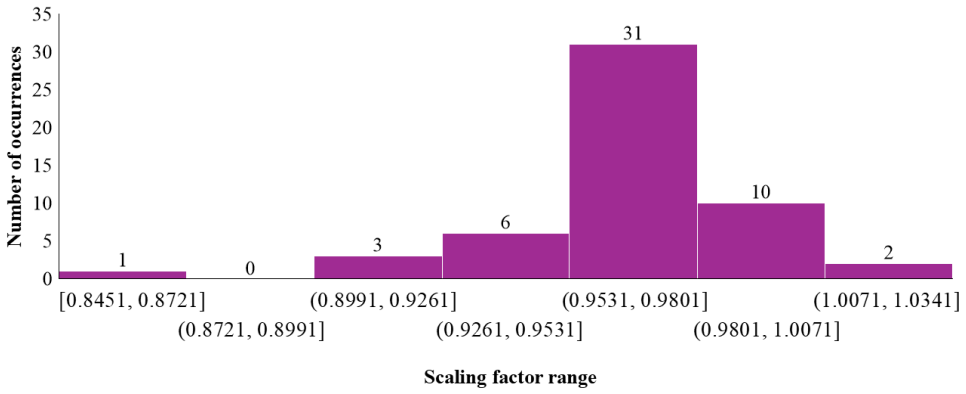

Figure 2. Histogram of correction factors, reported in the literature and presented in Table 2, of spectra in the infrared region for psychoactive substances. At the top of each column, the occurrence values for each range of values were indicated.

Lastly, it is worth highlighting some studies that have focused on more specific cases, demonstrating improved correlations between computational and experimental data when tailored correction factors are applied. For example, Fagan et al., 2021 [124] examined the structure of MDMA using correction factors that included the effect of solvation (D_2O and MeOD). In turn, Dobšíková et al. (2023) [83] derived correction factors for the vibrational spectra of amphetamine and methamphetamine. Additionally, scaling factors were applied to both high- and low-frequency regions of the IR spectrum for psychoactive substances across various classes: piperazine (1-amino-4-methylpiperazine) by Mahalakshmi & Balachandran (2015) [112], benzodiazepine (diazepam) by Mielcarek et al. (2011) [113], and Minaeva et al.

(2021) [93]. These targeted approaches underscore the effectiveness of using region-specific corrections to enhance the alignment of simulated and experimental spectra.

4. COMPARISON OF THEORETICAL AND EXPERIMENTAL SPECTRA

Obtaining experimental data for NPS is essential for validating theoretical spectra and can be achieved through two main approaches: in-house collection or reference databases.

The in-house collection allows researchers to standardize procedures and instrumentation, ensuring high-quality, reliable data. However, navigating regulatory restrictions can often complicate or hinder access to the necessary materials for analysis. In contrast, reference databases provide a more accessible alternative but come with their own challenges. These databases often lack detailed documentation on collection methods, and variations in instrumental specifications can affect the data reliability. Despite these limitations, reference databases offer the significant advantage of being readily available, often for no cost, avoiding the need for cumbersome government authorization. Moreover, local and institutional databases offer valuable data drawn from specific case occurrences, although they may not always be publicly accessible.

To address these challenges and enhance the availability of experimental data, significant efforts are being made to compile and optimize access to comprehensive resources. Two key initiatives in this area include:

SWGDRUG Database

Managed by the Scientific Working Group for the Analysis of Seized Drugs (SWGDRUG) [125], this database is a collaborative effort supported by contributions from the Drug Enforcement Administration (DEA) and the Special Testing and Research Laboratory (SFL1). It is periodically updated to include data on new or emerging drugs, primarily acquired through Fourier-transform infrared spectroscopy with attenuated total reflectance (FTIR-ATR). The database currently contains more than 830 spectra and includes essential details such as (i) compound form (salt or base), (ii) batch number of the sample, and (iii) date of spectrum entry into the database. The SWGDRUG database, therefore, serves as a critical resource for researchers and forensic analysts working with NPS.

ENFSI-DWG Database

The European Network of Forensic Science Institutes (ENFSI) Drugs Working Group (DWG) has been operational since 1997 and serves as a key resource for forensic analysis

(European Network of Forensic Science Institutes Drug Working Group (ENFSIDWG) 2024). The latest version (2024.05.08) of its database contains over 3,670 spectra. This repository provides detailed information about each compound, including: (i) various nomenclatures (e.g., typical/street names, IUPAC, InChI, InChIKey, molecular formula); (ii) compound form (salt, base, or not applicable); (iii) source (e.g., supplier or seizure); (iv) measurement type (e.g., KCl pellet, ATR, solid-phase GC-IR (gas chromatography infrared spectroscopy)); (v) sample preparation method (e.g., alkaline extract, solvents such as acetone, chloroform, ethanol, methanol, or direct measurements); (vi) general comments.

Both the ENFSI-DWG and SWGDRUG databases are built on experimental data and are widely used by forensic professionals worldwide as essential reference tools. However, a critical evaluation of these data is essential before they are adopted as references. These libraries may contain multiple spectra for the same molecule, but information regarding purity conditions is often not provided to users. For this reason, the use of univariate, multivariate, and probabilistic statistical analyses is recommended.

Table 2 compiles the primary methods for comparing spectra using different statistical approaches. The data show that most studies comparing theoretical and experimental spectra still focus on evaluating peak positions and signal intensities. While this method identifies specific spectral responses, it often neglects the overall spectrum. In most cases, no statistical treatment is applied. When statistical analyses are performed, they are often limited to univariate analysis or simple correlation studies, underscoring the need for more sophisticated approaches to improve data reliability and comparability.

Table 2. Statistical methods used to compare the spectroscopic responses obtained by theoretical and experimental data.

Statistical method	**Reference**
Intensity and characteristic signal	[43,53,55,81,83,85,86,93,94,101,107–114,117,119–121,127–129]
Binary method	[17,19,67,97]
Univariate and bivariate statistics	
RMS	[118]
MAE	[73,105]
Spearman's correlation coefficient	[95]
Pearson's correlation coefficient	[17,68,73,88,95,115,116]
Tanimoto coefficient or Jaccard index	[124]
Similarity/dissimilarity factor	[72,83,87]
Cosine similarity score	[64]
Kullback–Leibler (KL) divergence	[17,19,97]
Multivariate statistics	
Principal Component Analysis (PCA)	[17,19,66,67,88,97,98]
Hierarchical cluster analysis (HCA)	[17,97,98]

t-distributed Stochastic Neighbor Embedding (t-NSE)	[98]
Soft Independent Modelling of Class Analogies (SIMCA)	[19,66,67,97]
Partial Least Squares Discriminant Analysis (PLS-DA)	[68]

4.1.Univariate and bivariate statistical analyses

Univariate descriptive analysis focuses on describing and summarizing the properties of a dataset. This approach relies solely on the dataset under study to identify trends and draw conclusions, without making prior inferences about the general population. In the case of statistical analysis of spectroscopic responses applied to NPS, key metrics include: (i) measures of position (e.g., mean, median, mode, and percentiles); (ii) measures of dispersion or variability (e.g., range, standard deviation, standard error); (iii) measures of association (e.g., chi-square, Spearman's coefficient); and (iv) measures of correlation (e.g., Pearson's correlation coefficient) [106].

Bivariate analyses examine relationships between two variables, focusing on associations for qualitative data or correlations for quantitative data. Spearman's coefficient (r_{sp}) [130] measures the degree of association between ranked qualitative variables. For this analysis, the data must be ranked in ascending order, and the metric determines the difference (d_k) between rank orders (k) based on the number of observations (n), as described in **Equation 4**. Pearson's correlation coefficient [131] (**Equation 5**) is more suitable for quantitative variables. This statistical tool evaluates the linear relationship between two quantitative variables, including its intensity and direction [106,132].

$$r_{sp} = 1 - \frac{6\sum_{k=1}^{n} d_k^2}{n.(n^2-1)} \quad \textbf{(4)}$$

$$r = \frac{\sum_{i=1}^{n}(x_i - \bar{x}).(y_i - \bar{y})}{\sqrt{\sum_{i=1}^{n}(x_i - \bar{x})^2}.\sqrt{\sum_{i=1}^{n}(y_i - \bar{y})^2}} \quad \textbf{(5)}$$

Interpretations for both Spearman (association) and Pearson (correlation) coefficients follow a similar scale: (i) Perfect Association/Correlation: Values of 1 or −1 indicate a perfect positive or negative association/correlation, respectively; (ii) Very Strong Association/Correlation: Values between 0.90 and 0.99 (positive or negative) suggest a very strong relationship; (iii) Strong Association/Correlation: Values between 0.70 and 0.89 (positive or negative) indicate a strong relationship; (iv) Moderate Association/Correlation: Values between 0.50 and 0.69 (positive or negative) reflect a moderate relationship; (v) Weak Association/Correlation: Values between 0.20 and 0.49 (positive or negative) represent a weak relationship; (vi) No Significant Association/Correlation: Values below 0.20 suggest no

meaningful relationship [106,130,131]. Several studies have applied these coefficients to compare spectra, often presenting results visually through heatmaps (**Figure 3**). For notable examples, see Mariotto et al. (2024) and Rodrigues et al. (2022) [68,88].

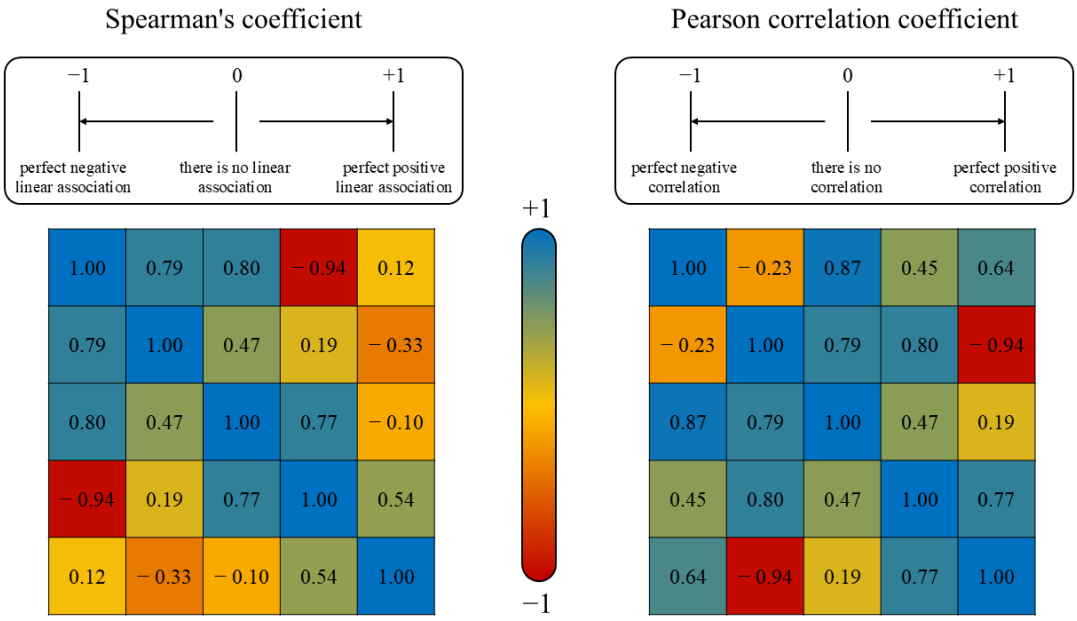

Figure 3. Illustrative representation of the creation of a heatmap and the interpretation of association (Spearman's coefficients) and correlation (Pearson's correlation coefficient) between the studied variables [130,131].

Building on this approach, He (2021) [95] investigated how correction factors and the three-dimensional structures of psychoactive substances influence these coefficients. The study revealed that scaling factors improved Pearson's correlation coefficients but had little effect on Spearman's coefficients. Notably, these comparative metrics highlighted that responses obtained via DFT may overestimate intensities (e.g., C–H bending bands below 1300 cm^{-1}) and/or underestimate intensities (e.g., C–H stretching bands above 2800 cm^{-1}) within the same spectrum.

Studies utilizing Pearson's correlation coefficient, revealed a strong correlation between experimental and theoretical data. However, experimental results consistently exhibited lower correlation coefficients than theoretical predictions for the same substance. These findings underscore the potential of computational approaches for generating infrared spectra of NPS, whether they are well-characterized or have minimal to no existing information [17,68,73,88,95,115,116]. Nonetheless, these statistical measures remain critical for validating and refining the alignment between theoretical and experimental spectra whenever feasible.

4.2. Similarity Scoring

Another method for assessing the agreement between theoretical and experimental spectroscopic responses is through the application of similarity scores. These measures assess how closely two spectra align, based on quantitative metrics such as the squared cosine similarity (**Equation 6**) [133] and the Tanimoto coefficient (also referred to as the Jaccard similarity coefficient, **Equation 7**) [134]. Both metrics have demonstrated comparable performance for this type of scoring [64].

$$S_c(A,B) := \cos(\theta) = \frac{A.B}{\|A\|\|B\|} = \frac{\sum_{i=1}^{n} A_i B_i}{\sqrt{\sum_{i=1}^{n}(A_i)^2}\sqrt{\sum_{i=1}^{n}(B_i)^2}} \quad \textbf{(6)}$$

$$J(A,B) = \frac{|A \cap B|}{|A \cup B|} = \frac{|A \cap B|}{|A| + |B| - |A \cap B|} \quad \textbf{(7)}$$

Cosine and Tanimoto similarity scores use vectors A and B, which represent finite sets of spectral samples. In both cases, the similarity scores ranging between 0 and 1 ($0 \leq S_c(A,B) \leq 1$ and $0 \leq J(A,B) \leq 1$). A similarity score of 1 indicates complete similarity, while a score of 0 occurs when the intersection of A and B is empty. The cosine similarity, $S_c(A,B)$, measures the cosine of the angle between vectors A and B, while the Tanimoto coefficient, $J(A,B)$, evaluates the ratio of the intersection to the union of sets A and B.

Houthuijs et al. (2023) [64] applied similarity factors to the spectra of drug metabolites, demonstrating a satisfactory trend in data comparisons. However, the authors highlighted the importance of cautious interpretation of absolute values, noting that these scores primarily reflect a recovery rate rather than a definitive measure of agreement. Similarly, Dobšíková et al. (2023) [83] analyzed the vibrational spectra of amphetamine and methamphetamine, employing similarity factors to assess the alignment of theoretical data with experimental results. Their study reported similarity scores of 0.75 for amphetamine and 0.84 for methamphetamine, indicating a reasonable degree of agreement.

Spálovská et al. (2019) [87] examined synthetic cathinones methylone and pentylone, focusing on their spectral profiles within the 1750–1250 cm^{-1} range. Using the CDSpecTech software [135], they obtained similarity indices of 0.85 for methylone and 0.91 for pentylone, showcasing a high level of consistency between the spectra.

4.3.Multivariate Analysis

Multivariate data analysis encompasses a set of statistical techniques designed to examine, identify patterns, interpret relationships, and make decisions based on the similarities

or divergences among multiple variables [136–139]. This analytical approach has become indispensable across diverse disciplines, including economics, psychology, engineering, and forensic science [140–142]. These methods can be broadly categorized based on the objectives of the analysis and the nature of the data, including: (i) exploratory analysis; (ii) dependency analysis; (iii) interdependency analysis; (iv) discriminant analysis; and (v) time-series analysis [106,143].

These categories allow for a more precise and effective selection of analytical methods, tailored to the structure and objectives of the evaluation. Principal Component Analysis (PCA), an exploratory and unsupervised method, is among the most widely used techniques. PCA reduces the dimensionality of datasets, making their interpretation and visualization more manageable [143,144]. Another common exploratory technique is Hierarchical Cluster Analysis (HCA), which uses a hierarchical process to group similar pairs of data points. This method often employs various linkage approaches, such as nearest neighbor or farthest neighbor. Like PCA, HCA progressively reduces the dimensionality of the data matrix until all data points are consolidated into a single cluster [143,145].

In supervised analyses, where prior information is utilized to organize or classify data, commonly used methods include: (i) Classification or Regression Trees, which segment data into decision-based branches; (ii) Neural Networks, which model complex relationships through interconnected layers; (iii) Partial Least Squares Regression (PLS), which relates predictors to responses in high-dimensional data; (iv) Partial Least Squares Discriminant Analysis (PLS-DA), a variant of PLS tailored for classification tasks; (v) SIMCA (Soft Independent Modeling of Class Analogies), which constructs classification models based on predefined classes; and other techniques [143–146]. Each method offers distinct features and analytical approaches to interpret results effectively.

4.4.Confusion matrix

A confusion matrix (**Figure 4**) is often employed to assess the robustness and accuracy of these models. This matrix compares actual and predicted classes, with the diagonal entries representing correct classifications. Additionally, it provides valuable metrics for evaluating regression and classification models, enhancing their reliability and interpretability.

		Prediction		
		Class 1	Class 2	Total
Indication	Class 1	TP	FP (Type I error)	TP + FP
	Class 2	FN (Type II error)	TN	FN + TN
	Total	TP + FN	FP + TN	TP + FP + FN + TN

Figure 4. Confusion or generic correspondence matrix, where green represents the correctly predicted values and red represents the incorrect class indications [147].

The confusion matrix is typically structured as a 2x2 table, containing the following classifications: (i) True Positives (TP): Samples correctly predicted as belonging to a class; (ii) False Negatives (FN): Samples that belong to a class but are incorrectly predicted as not belonging; (iii) False Positives (FP): Samples that do not belong to a class but are incorrectly predicted as belonging; (iv) True Negatives (TN): Samples correctly predicted as not belonging to a class.

Based on these values, several performance metrics can be calculated to evaluate model accuracy and robustness: (i) Sensitivity or Recall (**Equation 8**): Measures the ability to correctly identify true positives; (ii) Precision (**Equation 9**): Reflects the proportion of true positives among all positive predictions; (iii) Specificity (**Equation 10**): Indicates the ability to correctly identify true negatives; (iv) Accuracy or Efficiency (**Equation 11**): Represents the overall proportion of correct predictions; (v) F1-Score (**Equation 12**): A harmonic mean of precision and recall, balancing both metrics; (vi) Jaccard Index or Critical Success Index (**Equation 13**): Assesses the overlap between predicted and actual classes; (vii) Phi Coefficient or Matthews Correlation Coefficient (MCC) (**Equation 14**): A robust measure of correlation between predicted and actual values, considering all four matrix elements (TP, FN, FP, TN) [147–150]. These metrics provide comprehensive insights into model performance, with higher values indicating greater reliability and effectiveness.

$$\text{Sensitivity} = \frac{\text{TP}}{\text{TP} + \text{FN}} \quad \textbf{(8)}$$

$$\text{Precision} = \frac{\text{TP}}{\text{TP} + \text{FP}} \quad \textbf{(9)}$$

$$\text{Specificity} = \frac{\text{TN}}{\text{TN} + \text{FP}} \quad \textbf{(10)}$$

$$\text{Accuracy} = \frac{\text{TN} + \text{TP}}{\text{TN} + \text{FP} + \text{TP} + \text{FN}} \quad \textbf{(11)}$$

$$\text{F1-Score} = \frac{\text{TP}}{\text{TP} + \frac{1}{2}(\text{FP} + \text{FN})} \quad \textbf{(12)}$$

$$\text{Jaccard Index} = \frac{\text{TP}}{\text{TP} + \text{FN} + \text{FP}} \quad \textbf{(13)}$$

$$\text{MCC} = \frac{(\text{TP} \times \text{TN}) - (\text{FP} \times \text{FN})}{\sqrt{(\text{TP} + \text{FN}) \times (\text{FP} + \text{TN}) \times (\text{TP} + \text{FP}) \times (\text{FN} + \text{TN})}} \quad \textbf{(14)}$$

These parameters are expressed as ratios, typically analyzed on a scale from 0 to 1 or as percentages. A value closer to 1 or 100% signifies greater model robustness and reliability. Sensitivity measures the model's ability to correctly classify positive samples (minimizing Type II errors, or false negatives), while specificity evaluates its capacity to identify negative samples (minimizing Type I errors, or false positives), and detect misclassifications. Among the metrics, the F1-score, Jaccard Index, and MCC are particularly reliable for assessing model quality. These metrics are less prone to sampling bias and effectively account for Type I and Type II errors, providing a balanced evaluation of model performance [147,148,150].

4.5.Hit Quality Index

An IR spectrum typically consists of thousands of data points. Therefore, robust algorithms must effectively be employed to compare spectra. Among them, the Hit Quality Index (HQI) is a widely used numerical metric to assess the similarity between an unknown IR spectrum and reference spectra within a spectral library. HQI plays a crucial role in spectroscopic studies, particularly in identifying substances by matching unknown samples with known spectral profiles. By quantifying the degree of similarity, HQI simplifies the identification process based on IR spectral characteristics [151–153].

The HQI value is generated by comparing the unknown spectrum with each reference spectrum in the library, using mathematical calculations to assess their distance or similarity. Several mathematical methods support the derivation of HQI values, increasing their accuracy and reliability [65,154,155]. This metric is indispensable in analytical applications where accurate substance identification is critical.

4.6.Applications in NPS

Tcharkhetian et al. (2021) [17] investigated the synthetic cathinone α-pyrrolidinopentiophenone using statistical approaches to validate theoretical models against experimental data. A 2^3 factorial design optimized computational parameters, identifying the best DFT methods and basis sets. A Boltzmann distribution was used to determine the most probable conformers, and linear regression confirmed the alignment between simulated and experimental structural data. Multivariate techniques, including HCA and PCA, were applied to compare infrared spectra, while Kullback-Leibler divergence quantified their similarity. These approaches provided reliable validation for computational methods for forensic and analytical chemistry applications.

Sinhorini et al. (2021) [97] expanded on this work by studying multiple fentanyl analogs. A 2^4 factorial design was performed to optimize the DFT conditions, while PCA, HCA, and SIMCA validated clustering and classification of infrared spectra. Kullback-Leibler divergence was again employed to confirm the similarity between theoretical and experimental spectra.

Dogruer Erkok et al. (2024) [66] evaluated fentanyl analogs, focusing on 16 structures similar to 4-fluoroisobutyryl fentanyl (4-FIBF) and cyclopropyl fentanyl (CPrF). Their findings indicated that 4-FIBF and CPrF were distinctly separated from other analogs, with cyclic structures clustering together. Additionally, the spectral peaks with the highest intensities were identified as key factors in forming these groupings.

Supervised classification models were also developed in other studies. Castro et al. (2020) [67] and Bruni et al. (2018) [19] applied the SIMCA method to develop classification models for synthetic cannabinoids and amphetamine-like stimulants, respectively. Both studies demonstrated the effectiveness of SIMCA in classifying infrared spectra of NPS using computational approaches. Rodrigues et al. (2022)[68] took a different approach by applying PLS-DA to create regression models based on theoretical data, predicting experimental results. Their study focused on determining whether seized samples corresponded to the synthetic cathinone N-ethylpentylone. In addition to regression methods, the authors used a confusion matrix to evaluate their models.

These studies, along with those summarized in **Table 2**, underscore the necessity of using statistical methods to support decision-making, particularly when a new substance is detected, and its structural class is unknown. As highlighted by Pacheco & Correa (2023) [156], who conducted a bibliometric analysis on the application of statistical methods to psychoactive substances, univariate and multivariate statistical analyses, as well as machine learning, will increasingly play a vital role in understanding psychoactive substances, whether they are newly discovered or subject to regulatory control.

5. CHALLENGES AND PERSPECTIVES

Despite rigorous precautions and adherence to good laboratory practices, several experimental factors can complicate comparisons between theoretical and experimental spectroscopic responses. Interference and noise can result in false positives or negatives depending on how the spectra are acquired. If there is an air gap between the NPS sample and the analyzer, deviations in band intensity may occur, particularly at shorter wavelengths [115]. Corrections allowed by the ATR method can mitigate this effect if the sample surface is optically flat. However, the observed reduction is not necessarily proportional to the wavelength [10,157–159].

Another challenge arises from the composition of NPS, which are often mixtures of multiple substances, including adulterants or contaminants [160,161]. These mixtures can complicate substance identification, as they may amplify spectroscopic signals beyond what is expected for pure substances [162]. Furthermore, many NPS share similar chemical backbones, such as amphetamines, cathinones, NBOH, and NBOMes. This structural similarity can lead to preliminary misidentifications if the spectra of all mixture components are not taken into account [115,163]. In such cases, computational methods can serve as a reference standard, as they generate spectra under idealized conditions where the molecule is isolated, producing "pure" chemical responses.

However, real-world samples are rarely isolated, and non-covalent interactions within mixtures and between molecules can significantly influence spectroscopic responses, an area still underexplored. Džodić et al. (2024) [73] conducted a theoretical analysis (M05-2X/6-31+G(d,p)) of dimers involving a benzodiazepine family structure and common adulterants and diluents reported in seizures. Similarly, Minaeva et al. (2021) [93] evaluated the dimerization patterns of 4-methyl methcathinone (4-MMC) and its spectroscopic responses in the gas phase and solid state using computational methods. The authors reported a satisfactory correlation between the simulations, highlighting that interpreting solid-state spectra required careful consideration due to frequency shifts and new bands caused by the crystalline phase.

Another complicating factor is the common presence of NPS in salt forms, such as hydrochlorides or sulfates. These counterions affect the spectra, and their accurate simulation is complex but essential for matching experimental data. For example, Houthuijs et al. (2023) [64] studied protonated and deprotonated ions through multi-step simulations, combining PM6 conformational searches (filtering structures with energy differences higher than 40 kJ mol^{-1}), B3LYP/6-311+G(d,p) frequency calculations, and MP2/6-311+G(d,p) optimizations for thermodynamic parameters. This approach yielded frequencies and physicochemical

parameters closely aligned with experimental values, effectively providing key information about drug metabolites.

Graf et al. (2020) [53] reported that amphetamine salts are predominantly found as sulfates, which exhibit unique spectral characteristics that help distinguish them from their chloride counterparts. The authors performed a conformational search for various simulated crystalline compounds, including amphetamine, methamphetamine, MDA, MDMA, and substituted methcathinones. Their findings revealed that the angles of interactions between protonated amines and chloride ions consistently ranged from 160 to 180 degrees. This structural feature aids in obtaining more accurate spectral predictions, as secondary amine bonds are elongated due to hydrogen bonding, resulting in more intense peaks between 2500 and 2900 cm^{-1}.

Recent advances in artificial intelligence (AI) have transformed infrared spectral analysis. Generative AI models can rapidly predict IR spectra from molecular structures, incorporating anharmonic effects and providing faster alternatives to conventional computational methods [164]. Additionally, a notable advancement driven by AI is the development of extensive databases containing thousands of spectra. These prediction engines are based on empirical FTIR data, offering a powerful resource for analyzing compounds with limited or unavailable experimental data [165]. Emerging technologies like attention-based graph neural networks (e.g., AttentiveFP) further enhance predictive accuracy by employing advanced techniques to model IR spectra from chemical structures [166].

5.1. SWOT ANALYSIS

Theoretical methods have become indispensable for obtaining spectroscopic data on NPS, offering a way to provide solutions to challenges faced by the emergence of these compounds. Combining computational and statistical methods can provide a tool for helping to predict the properties of these drugs. In this scenario, we have performed a SWOT (Strengths, Weaknesses, Opportunities, and Threats) analysis to enhance understanding and strategic planning. This analysis evaluates the potential of these methods in generating spectroscopic patterns for NPS, providing key takeaways with the potential to bridge past research with emerging directions and trends [167,168].

SWOT analysis, widely recognized for its strategic value in corporate and industrial contexts, has also been applied across various research fields. These include natural product research [167], supercapacitors [169], cheminformatics as an educational tool in STEM [170],

chemometric methods in forensic chemistry [168], and metabolomic analysis of environmental data [171].

Figure 5 summarizes the SWOT analysis, dividing them into four strategic categories. This framework provides a comprehensive overview of the internal and external factors influencing the use of computational methods for NPS, along with their potential opportunities and challenges.

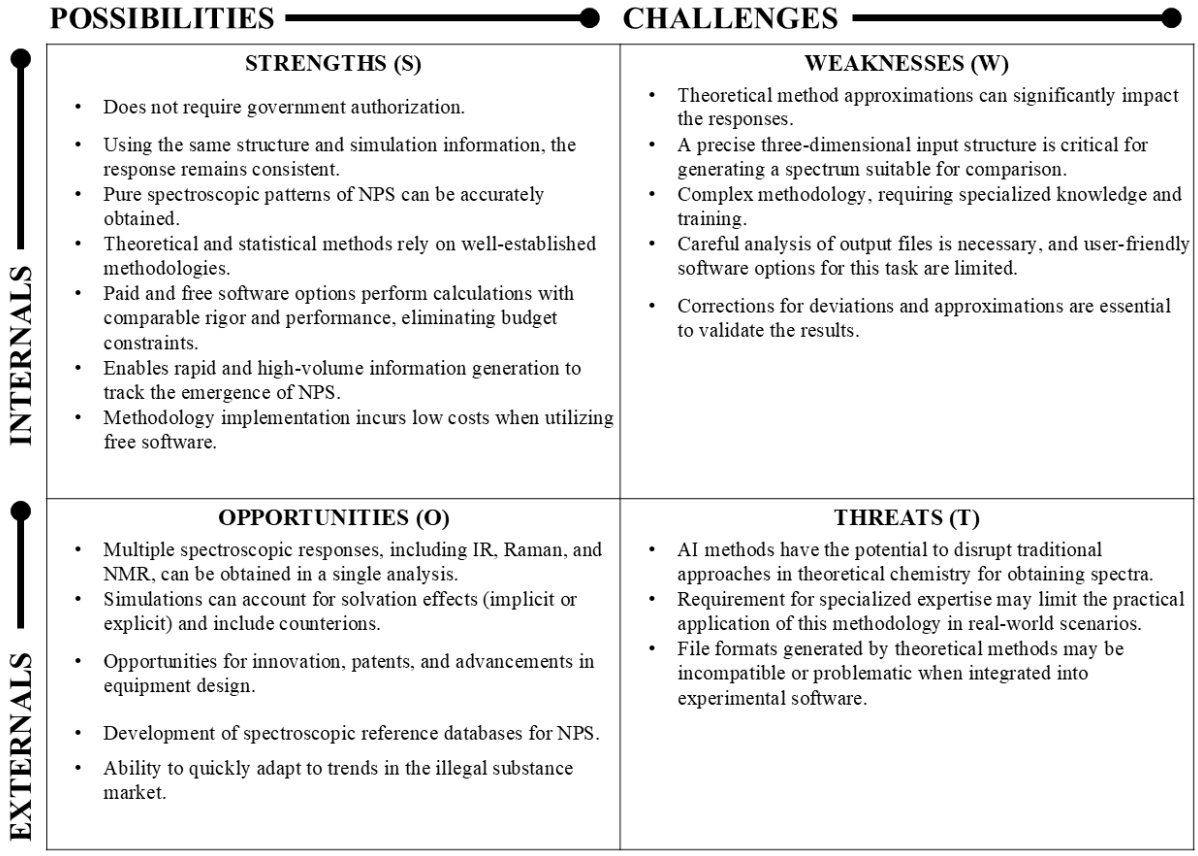

Figure 5. SWOT analysis for the application of theoretical methods to obtain NPS spectroscopic data.

As highlighted in **Figure 5**, while promising progress has been made, considerable advancements are still required before computational methods can reliably predict experimental data with high confidence. The forensic field related to NPS presents a particularly promising opportunity, delivering encouraging results. However, achieving stronger correlations and broader applications remains a significant challenge in advancing the use of these methods for NPS analysis.

CONCLUSIONS

This study underscores the indispensable role of theoretical chemistry in predicting and interpreting the spectroscopic properties of NPS. When complemented by systematic

conformational analysis and post-processing techniques to mitigate inherent methodological limitations, density functional theory (DFT) can produce highly accurate computationally predicted infrared spectra that serve as reliable references for experimental data. This is particularly effective when computations are meticulously designed, with careful selection of DFT functionals, basis sets, and the inclusion of additional parameters such as solvent effects and counterions when necessary. The integration of statistical methods, including multivariate analyses and similarity scoring, enhances the validation process and facilitates the accurate identification and classification of NPS in real-world samples. This approach effectively addresses challenges such as structural similarities among compounds from different classes and the presence of complex mixtures containing adulterants typically found in real samples.

The application of scaling factors and statistical corrections derived from rigorous analysis can lead to a better match between theoretical spectra and experimental results, improving the reliability of spectral databases. This is particularly crucial when dealing with NPS that have minimal prior information or when experimental data are scarce or difficult to obtain due to legal and ethical constraints.

The advent of machine learning and artificial intelligence offers the opportunity to automate and refine spectral predictions by utilizing large data sets to improve model training and validation. Therefore, the integration of artificial intelligence and the development of extensive spectral databases hold great promise but must be pursued cautiously to maintain analytical integrity and reliability. Addressing these limitations requires meticulous attention to data quality, algorithmic transparency, and validation through interdisciplinary collaboration.

As NPS continue to evolve, the timely and accurate identification of these substances is critical for public health and safety. Developing open-access databases and sharing knowledge across international borders can enhance collective efforts to combat the spread of NPS. Investment in training programs and user-friendly computational tools can democratize access to these advanced methods, enabling a broader range of laboratories and agencies to implement them effectively.

This integrated approach holds promise for more effective monitoring, identification, and regulation of NPS. Through the use of theoretical chemistry, robust statistical analyses and new AI technologies, we can develop more reliable and comprehensive methods for the detection and characterization of NPS. This will ultimately contribute to public health initiatives, aid law enforcement efforts, and inform policy decisions, ensuring a proactive response to the ever-changing landscape of psychoactive substances.

Declaration of AI and AI-assisted technologies in the writing process

During the preparation of this work, the authors used GPT 4o and Grammarly to perform translation actions and improve flow, readability and organization. After using this tool/service, the authors reviewed and edited the content as needed and take full responsibility for the content of the publication.

REFERENCES

[1] H.-H. Chou, C.-H. Hsieh, C.-H. Chaou, C.-K. Chen, T.-H. Yen, S.-C. Liao, C.-J. Seak, H.-Y. Chen, Synthetic cathinone poisoning from ingestion of drug-laced “instant coffee packets” in Taiwan, Hum Exp Toxicol 40 (2021) 1403–1412. https://doi.org/10.1177/0960327121996043.

[2] United Nations Office on Drugs and Crime, Drug market trends: Cocaine, amphetamine-type stimulants, new psychoactive substances, in: United Nations Office on Drugs and Crime (Ed.), World Drug Report 2022, United Nations publication, Vienna, 2022: pp. 1–111. https://www.unodc.org/res/wdr2022/MS/WDR22_Booklet_4.pdf (accessed July 28, 2022).

[3] A.J. Krotulski, Challenges in Identifying Novel Psychoactive Substances and a Stronger Path Forward, National Institute of Justice (2022). https://nij.ojp.gov/topics/articles/challenges-identifying-novel-psychoactive-substances-and-stronger-path-forward (accessed January 25, 2024).

[4] United Nations Publication, World Drug Report: Executive Sumary, United Nations publication, Sales No. E.23.XI.7, Vienna, 2023. https://www.unodc.org/res/WDR-2023/WDR23_Exsum_fin_SP.pdf (accessed January 14, 2024).

[5] M.F. Custódio, L.O. Magalhães, L.C. Arantes, J.W.B. Braga, Identification of synthetic drugs on seized blotter papers using ATR-FTIR and PLS-DA: Routine application in a forensic laboratory, J Braz Chem Soc 32 (2021) 513–522. https://doi.org/10.21577/0103-5053.20200205.

[6] Scientific Working Group for the Analysis of Seized Drugs (SWGDRUG), Recommendations: Code of Professional Practice, Education and Training, Methods of Analysis, and Quality Assurance. Version 8.1, 2022.

[7] A. Rohman, A. Windarsih, M.A.M. Hossain, M.R. Johan, Md.E. Ali, N.A. Fadzilah, Application of near- and mid-infrared spectroscopy combined with chemometrics for discrimination and authentication of herbal products: A review, J Appl Pharm Sci 9 (2019) 137–147. https://doi.org/10.7324/JAPS.2019.90319.

[8] M. Manley, V. Baeten, Spectroscopic Technique: Near Infrared (NIR) Spectroscopy, in: Modern Techniques for Food Authentication, Elsevier, 2018: pp. 51–102. https://doi.org/10.1016/B978-0-12-814264-6.00003-7.

[9] K.B. Beć, J. Grabska, C.W. Huck, NIR spectroscopy of natural medicines supported by novel instrumentation and methods for data analysis and interpretation, J Pharm Biomed Anal 193 (2021) 113686. https://doi.org/10.1016/j.jpba.2020.113686.

[10] D.L. Pavia, G.M.; Lampman, G.S.; Kriz, J.A. Vyvyan, Introduction to Spectroscopy, 4th ed, Cengage Learning, 2008.

[11] I.N. Levine, Quantum chemistry, 6th ed., Pearson Prentice Hall, London (UK), 2009. https://doi.org/10.1007/s00205-003-0281-6.

[12] Yong-Cheng Ning, Interpretation of Infrared Spectra, in: Yong-Cheng Ning (Ed.), Interpretation of Organic Spectra, Wiley, 2011: pp. 129–146. https://doi.org/10.1002/9780470825181.ch5.

[13] J. Coates, Interpretation of Infrared Spectra, A Practical Approach, in: Encyclopedia of Analytical Chemistry, John Wiley & Sons, Ltd, Chichester, UK, 2006. https://doi.org/10.1002/9780470027318.a5606.

[14] R. Sutherland, R. Bruno, A. Peacock, S. Lenton, A. Matthews, C. Salom, P. Dietze, K. Butler, L. Burns, M.J. Barratt, Motivations for new psychoactive substances use among regular psychostimulant users in Australia, International Journal of Drug Policy 43 (2017) 23–32.

[15] A. Kloosterman, A. Mapes, Z. Geradts, E. van Eijk, C. Koper, J. van den Berg, S. Verheij, M. van der Steen, A. van Asten, The interface between forensic science and technology: how technology could cause a paradigm shift in the role of forensic institutes in the criminal justice system, Philosophical Transactions of the Royal Society B: Biological Sciences 370 (2015) 20140264. https://doi.org/10.1098/rstb.2014.0264.

[16] V. Barone, S. Alessandrini, M. Biczysko, J.R. Cheeseman, D.C. Clary, A.B. McCoy, R.J. DiRisio, F. Neese, M. Melosso, C. Puzzarini, Computational molecular spectroscopy, Nature Reviews Methods Primers 1 (2021) 38. https://doi.org/10.1038/s43586-021-00034-1.

[17] A.E.G. Tcharkhetian, A.T. Bruni, C.H.P. Rodrigues, Combining experimental and theoretical approaches to study the structural and spectroscopic properties of Flakka (α-pyrrolidinopentiophenone), Results Chem 3 (2021) 100254. https://doi.org/10.1016/j.rechem.2021.100254.

[18] C.H.P. Rodrigues, V.B.P. Leite, A.T. Bruni, Can NMR spectroscopy discriminate between NPS amphetamines and cathinones? An evaluation by in silico studies and chemometrics, Chemometrics and Intelligent Laboratory Systems 210 (2021) 104265. https://doi.org/10.1016/j.chemolab.2021.104265.

[19] A.T. Bruni, P.O.M. de Carvalho, C.H.P. Rodrigues, V.B.P. Leite, In silico methods in forensic science: Quantum chemistry and multivariate analysis applied to infrared spectra of new amphetamine- and cathinone-derived psychoactive substances, Forensic Chemistry 9 (2018) 21–34. https://doi.org/10.1016/j.forc.2018.03.006.

[20] R. Custodio, N.H. Morgon, The Density-Functional Theory, Quim Nova 18 (1995) 44–55.

[21] A. Omotayo, A.K. Oyebamiji, O.R. Oyewole, B. Semire, A DFT-Based QSAR and Molecular Docking Studies on Potent Anti-Colon Cancer Activity of Pyrazole Derivatives, Global Journal of Medical Research:B Pharma, Drug Discovery, Toxicology & Medicine 18 (2018) 9–21.

[22] N.S. Babu, DFT studies of molecular structure , equilibrium constant for keto-enol tautomerism and geometrical isomerism (E-Z) of 2-amino-1-phenylpropan-1- one (Cathinone), Pelagia Research Library 4 (2013) 147–153.

[23] A. Pietropolli Charmet, Y. Cornaton, Benchmarking fully analytic DFT force fields for vibrational spectroscopy: A study on halogenated compounds, J Mol Struct 1160 (2018) 455–462. https://doi.org/10.1016/j.molstruc.2018.01.089.

[24] C.J. Cramer, D.G. Truhlar, Theoretical Chemistry Accounts, Springer Berlin Heidelberg, Berlin, Heidelberg, 2001. https://doi.org/10.1007/978-3-662-10421-7.

[25] P. Hohenberg, W. Kohn, Inhomogeneous Electron Gas, Physical Review 136 (1964) 864–871. https://doi.org/10.1103/PhysRevB.7.1912.

[26] W. Kohn, L.J. Sham, Self-Consistent Equations Including Exchange and Correlation Effects, Physical Review 140 (1965) A1133–A1138. https://doi.org/10.1103/PhysRev.140.A1133.

[27] D.A. McQuarrie, J.D. Simon, Physical chemistry: a molecular approach, University Science Books, Sausalito, Calif., 1997.

[28] E.G. Lewars, Computational Chemistry: Introduction to the Theory and Applications of Molecular and Quantum Mechanics, Second Edi, Springer, Ontario, Canada, 2011. https://doi.org/10.1007/978-90-481-3862-3.

[29] C.J. Cramer, Essentials of Computational Chemistry Theories and Models, 2004. https://doi.org/10.1021/ci010445m.

[30] P. Atkins, J. de Paula, J. Keeler, Physical Chemistry, 11th edition, Oxford University Press, Oxford, 2018.

[31] J.B. Foresman, Ae. Frisch, Exploring Chemistry With Electronic Structure Methods, 3rd ed., Wallingford, CT, 2015. https://gaussian.com/expchem3/ (accessed November 22, 2024).

[32] A.M. Teale, T. Helgaker, A. Savin, C. Adamo, B. Aradi, A. V. Arbuznikov, P.W. Ayers, E.J. Baerends, V. Barone, P. Calaminici, E. Cancès, E.A. Carter, P.K. Chattaraj, H. Chermette, I. Ciofini, T.D. Crawford, F. De Proft, J.F. Dobson, C. Draxl, T. Frauenheim, E. Fromager, P. Fuentealba, L. Gagliardi, G. Galli, J. Gao, P. Geerlings, N. Gidopoulos, P.M.W. Gill, P. Gori-Giorgi, A. Görling, T. Gould, S. Grimme, O. Gritsenko, H.J.A. Jensen, E.R. Johnson, R.O. Jones, M. Kaupp, A.M. Köster, L. Kronik, A.I. Krylov, S. Kvaal, A. Laestadius, M. Levy, M. Lewin, S. Liu, P.-F. Loos, N.T. Maitra, F. Neese, J.P. Perdew, K. Pernal, P. Pernot, P. Piecuch, E. Rebolini, L. Reining, P. Romaniello, A. Ruzsinszky, D.R. Salahub, M. Scheffler, P. Schwerdtfeger, V.N. Staroverov, J. Sun, E. Tellgren, D.J. Tozer, S.B. Trickey, C.A. Ullrich, A. Vela, G. Vignale, T.A. Wesolowski, X. Xu, W. Yang, DFT exchange: sharing perspectives on the workhorse of quantum chemistry and materials science, Physical Chemistry Chemical Physics 24 (2022) 28700–28781. https://doi.org/10.1039/D2CP02827A.

[33] K.R. Bryenton, A.A. Adeleke, S.G. Dale, E.R. Johnson, Delocalization error: The greatest outstanding challenge in density-functional theory, WIREs Computational Molecular Science 13 (2023). https://doi.org/10.1002/wcms.1631.

[34] S. Vuckovic, A. Gerolin, K.J. Daas, H. Bahmann, G. Friesecke, P. Gori-Giorgi, Density functionals based on the mathematical structure of the strong-interaction limit of DFT, WIREs Computational Molecular Science 13 (2023). https://doi.org/10.1002/wcms.1634.

[35] A.D. Becke, Density-functional exchange-energy approximation with correct asymptotic behavior, Phys Rev A (Coll Park) 38 (1988) 3098–3100. https://doi.org/10.1103/PhysRevA.38.3098.

[36] C. Lee, W. Yang, R.G. Parr, Development of the Colle-Salvetti correlation-energy formula into a functional of the electron density, Phys Rev B 37 (1988) 785–789. https://doi.org/10.1103/PhysRevB.37.785.

[37] P. Politzer, Jorge. Seminario, eds., Modern Density Functional Theory: A Tool for Chemistry, 1st ed., Elsevier Science, Texas (USA), 1995.

[38] J.C. Slater, Atomic shielding constants, Physical Review 36 (1930). https://doi.org/10.1103/PhysRev.36.57.

[39] C. De Oliviera, Método de Hartree-Fock, (2015) 1–9.

[40] R. Ditchfield, W.J. Hehre, J.A. Pople, Self-consistent molecular-orbital methods. IX. An extended gaussian-type basis for molecular-orbital studies of organic molecules, J Chem Phys 54 (1971). https://doi.org/10.1063/1.1674902.

[41] T. Clark, J. Chandrasekhar, G.W. Spitznagel, P.V.R. Schleyer, Efficient diffuse function-augmented basis sets for anion calculations. III. The 3-21+G basis set for first-row elements, Li–F, J Comput Chem 4 (1983). https://doi.org/10.1002/jcc.540040303.

[42] W.J. Hehre, R. Ditchfield, J.A. Pople, Self—Consistent Molecular Orbital Methods. XII. Further Extensions of Gaussian—Type Basis Sets for Use in Molecular Orbital Studies of Organic Molecules, J Chem Phys 56 (1972) 2257–2261. https://doi.org/10.1063/1.1677527.

[43] C.D. Zeinalipour-Yazdi, A DFT study of the interaction of aspirin, paracetamol and caffeine with one water molecule, J Mol Model 28 (2022) 285. https://doi.org/10.1007/s00894-022-05258-w.

[44] M.J. Frisch, J.A. Pople, J.S. Binkley, Self-consistent molecular orbital methods 25. Supplementary functions for Gaussian basis sets, J Chem Phys 80 (1984) 3265–3269. https://doi.org/10.1063/1.447079.

[45] A.J. Sadlej, Medium-size polarized basis sets for high-level-correlated calculations of molecular electric properties, Theor Chim Acta 81 (1992) 339–354. https://doi.org/10.1007/BF01118573.

[46] T.H. Dunning, Gaussian basis sets for use in correlated molecular calculations. I. The atoms boron through neon and hydrogen, J Chem Phys 90 (1989) 1007–1023. https://doi.org/10.1063/1.456153.

[47] P.J. Hay, W.R. Wadt, Ab initio effective core potentials for molecular calculations. Potentials for K to Au including the outermost core orbitale, J Chem Phys 82 (1985). https://doi.org/10.1063/1.448975.

[48] W.R. Wadt, P.J. Hay, Ab initio effective core potentials for molecular calculations. Potentials for main group elements Na to Bi, J Chem Phys 82 (1985). https://doi.org/10.1063/1.448800.

[49] D. Andrae, U. Häußermann, M. Dolg, H. Stoll, H. Preuß, Energy-adjusted ab initio pseudopotentials for the second and third row transition elements, Theor Chim Acta 77 (1990). https://doi.org/10.1007/BF01114537.

[50] A. Schäfer, H. Horn, R. Ahlrichs, Fully optimized contracted Gaussian basis sets for atoms Li to Kr, J Chem Phys 97 (1992) 2571–2577. https://doi.org/10.1063/1.463096.

[51] F. Weigend, R. Ahlrichs, Balanced basis sets of split valence, triple zeta valence and quadruple zeta valence quality for H to Rn: Design and assessment of accuracy, Physical Chemistry Chemical Physics 7 (2005) 3297. https://doi.org/10.1039/b508541a.

[52] H. Damasceno, A.M. Bassini, Espectroscopia, CienTec-USP (2021). https://parquecientec.usp.br/passeio-virtual/tudo-sao-ondas/espectroscopia (accessed January 31, 2023).

[53] W.F. Graf, J.R. Pearson, D.R.T. Appadoo, E.G. Robertson, C. Ennis, Synchrotron far-infrared spectra for the characterisation of molecular crystals of forensic interest: Amphetamine, methamphetamine, MDA, MDMA and substituted methcathinones, Vib Spectrosc 110 (2020) 103115. https://doi.org/10.1016/j.vibspec.2020.103115.

[54] M. Bursch, J. Mewes, A. Hansen, S. Grimme, Best-Practice DFT Protocols for Basic Molecular Computational Chemistry**, Angewandte Chemie International Edition 61 (2022). https://doi.org/10.1002/anie.202205735.

[55] W.F. Graf, J.R. Pearson, D.R.T. Appadoo, E.G. Robertson, C. Ennis, The prediction of far-infrared spectra for molecular crystals of forensic interest – Phenylethylamine, ephedrine & pseudoephedrine, Forensic Chemistry 17 (2020) 100204. https://doi.org/10.1016/j.forc.2019.100204.

[56] C.E. Tzeliou, M.A. Mermigki, D. Tzeli, Review on the QM/MM Methodologies and Their Application to Metalloproteins, Molecules 27 (2022) 2660. https://doi.org/10.3390/molecules27092660.

[57] X. Liao, R. Lu, L. Xia, Q. Liu, H. Wang, K. Zhao, Z. Wang, Y. Zhao, Density Functional Theory for Electrocatalysis, ENERGY & ENVIRONMENTAL MATERIALS 5 (2022) 157–185. https://doi.org/10.1002/eem2.12204.

[58] S. Ahmadi, A. Rezae, S. Ghosh, A. Malloum, A. Banach, A review on bioelectrochemical systems for emerging pollutants remediation: A computational approaches, J Environ Chem Eng 11 (2023) 110021. https://doi.org/10.1016/j.jece.2023.110021.

[59] Q. Liang, S. Wang, Y. Yao, P. Dong, H. Song, Transition Metal Compounds Family for Li–S Batteries: The DFT-Guide for Suppressing Polysulfides Shuttle, Adv Funct Mater 33 (2023). https://doi.org/10.1002/adfm.202300825.

[60] N. Ye, Z. Yang, Y. Liu, Applications of density functional theory in COVID-19 drug modeling, Drug Discov Today 27 (2022) 1411–1419. https://doi.org/10.1016/j.drudis.2021.12.017.

[61] B. Huang, G.F. von Rudorff, O.A. von Lilienfeld, The central role of density functional theory in the AI age, Science (1979) 381 (2023) 170–175. https://doi.org/10.1126/science.abn3445.

[62] S. Kaya, A. Thakur, A. Kumar, The role of in Silico/DFT investigations in analyzing dye molecules for enhanced solar cell efficiency and reduced toxicity, J Mol Graph Model 124 (2023) 108536. https://doi.org/10.1016/j.jmgm.2023.108536.

[63] S.-C. Liu, X.-R. Zhu, D.-Y. Liu, D.-C. Fang, DFT calculations in solution systems: solvation energy, dispersion energy and entropy, Physical Chemistry Chemical Physics 25 (2023) 913–931. https://doi.org/10.1039/D2CP04720A.

[64] K.J. Houthuijs, G. Berden, U.F.H. Engelke, V. Gautam, D.S. Wishart, R.A. Wevers, J. Martens, J. Oomens, An In Silico Infrared Spectral Library of Molecular Ions for Metabolite Identification, Anal Chem 95 (2023) 8998–9005. https://doi.org/10.1021/acs.analchem.3c01078.

[65] B. Lavine, J. Almirall, C. Muehlethaler, C. Neumann, J. Workman, Criteria for comparing infrared spectra – A review of the forensic and analytical chemistry literature, Forensic Chemistry 18 (2020) 100224. https://doi.org/10.1016/j.forc.2020.100224.

[66] S. Dogruer Erkok, E. Hernandez, J. Cruz, A.M. Mebel, B. McCord, Differentiating Structurally Similar Fentanyl Analogs by Comparing Density Functional Theory (DFT) Calculations and Surface-Enhanced Raman Spectroscopy (SERS) Results, Appl Spectrosc 78 (2024) 667–679. https://doi.org/10.1177/00037028241246010.

[67] J.S. de Castro, C.H.P. Rodrigues, A.T. Bruni, In Silico Infrared Characterization of Synthetic Cannabinoids by Quantum Chemistry and Chemometrics, J Chem Inf Model 60 (2020) 2100–2114. https://doi.org/10.1021/acs.jcim.9b00871.

[68] C.H.P. Rodrigues, R. de O. Mascarenhas, A.T. Bruni, In Silico Infrared Spectroscopy as a Benchmark for Identifying Seized Samples Suspected of Being N-Ethylpentylone, Psychoactives 2 (2022) 1–22. https://doi.org/10.3390/psychoactives2010001.

[69] J. Da Chai, M. Head-Gordon, Long-range corrected hybrid density functionals with damped atom-atom dispersion corrections, Physical Chemistry Chemical Physics 10 (2008). https://doi.org/10.1039/b810189b.

[70] N.M. Kreienborg, C. Merten, How to treat C–F stretching vibrations? A vibrational CD study on chiral fluorinated molecules, Physical Chemistry Chemical Physics 21 (2019) 3506–3511. https://doi.org/10.1039/C8CP02395F.

[71] Y. Zhao, D.G. Truhlar, The M06 suite of density functionals for main group thermochemistry, thermochemical kinetics, noncovalent interactions, excited states, and transition elements: Two new functionals and systematic testing of four M06-class functionals and 12 other function, Theor Chem Acc 120 (2008) 215–241. https://doi.org/10.1007/s00214-007-0310-x.

[72] K. Dobšíková, Ž. Javorská, M. Paškan, D. Spálovská, P. Trembulaková, J. Herciková, M. Kuchař, V. Kozmík, M. Kohout, V. Setnička, Enantioseparation and a comprehensive spectroscopic analysis of novel synthetic cathinones laterally substituted with a trifluoromethyl group, Spectrochim Acta A Mol Biomol Spectrosc 291 (2023) 122320. https://doi.org/10.1016/j.saa.2023.122320.

[73] J. Džodić, M. Marković, D. Milenković, D. Dimić, Molecular Aspects of the Interactions between Selected Benzodiazepines and Common Adulterants/Diluents: Forensic Application of Theoretical Chemistry Methods, Int J Mol Sci 25 (2024) 10087. https://doi.org/10.3390/ijms251810087.

[74] Y. Zhao, N.E. Schultz, D.G. Truhlar, Design of density functionals by combining the method of constraint satisfaction with parametrization for thermochemistry, thermochemical kinetics, and noncovalent interactions, J Chem Theory Comput 2 (2006). https://doi.org/10.1021/ct0502763.

[75] S. Grimme, J. Antony, S. Ehrlich, H. Krieg, A consistent and accurate *ab initio* parametrization of density functional dispersion correction (DFT-D) for the 94 elements H-Pu, J Chem Phys 132 (2010) 154104. https://doi.org/10.1063/1.3382344.

[76] S. Grimme, S. Ehrlich, L. Goerigk, Effect of the damping function in dispersion corrected density functional theory, J Comput Chem 32 (2011) 1456–1465. https://doi.org/10.1002/jcc.21759.

[77] E. Caldeweyher, S. Ehlert, A. Hansen, H. Neugebauer, S. Spicher, C. Bannwarth, S. Grimme, A generally applicable atomic-charge dependent London dispersion correction, Journal of Chemical Physics 150 (2019). https://doi.org/10.1063/1.5090222.

[78] T. Lewis-Atwell, P.A. Townsend, M.N. Grayson, Comparisons of different force fields in conformational analysis and searching of organic molecules: A review, Tetrahedron 79 (2021) 131865. https://doi.org/10.1016/j.tet.2020.131865.

[79] A.T. Bruni, M.M.C. Ferreira, Theoretical study of omeprazole behavior: Racemization barrier and decomposition reaction, Int J Quantum Chem 108 (2008) 1097–1106. https://doi.org/10.1002/qua.21597.

[80] A.T. Bruni, V.B.P. Leite, M.M.C. Ferreira, Conformational analysis: A new approach by means of chemometrics, J Comput Chem 23 (2002) 222–236. https://doi.org/10.1002/jcc.10004.

[81] P. Bhadoria, V. Ramanathan, Conformational Landscape and Properties of Psilocybin: A Computational Approach, ChemistrySelect 7 (2022). https://doi.org/10.1002/slct.202203026.

[82] W. Kolodziejczyk, J. Jodkowski, T.M. Holmes, G.A. Hill, Conformational analysis of flephedrone using quantum mechanical models, J Mol Model 19 (2013) 1451–1458. https://doi.org/10.1007/s00894-012-1673-z.

[83] K. Dobšíková, P. Michal, D. Spálovská, M. Kuchař, N. Paškanová, R. Jurok, J. Kapitán, V. Setnička, Conformational analysis of amphetamine and methamphetamine: a comprehensive approach by vibrational and chiroptical spectroscopy, Analyst 148 (2023) 1337–1348. https://doi.org/10.1039/D2AN02014A.

[84] V. Lukić, R. Micić, B. Arsić, B. Nedović, Ž. Radosavljević, Overview of the major classes of new psychoactive substances, psychoactive effects, analytical determination and conformational analysis of selected illegal drugs, Open Chem 19 (2021) 60–106. https://doi.org/10.1515/chem-2021-0196.

[85] M. Baranska, J.Cz. Dobrowolski, A. Kaczor, K. Chruszcz-Lipska, K. Gorz, A. Rygula, Tobacco alkaloids analyzed by Raman spectroscopy and DFT calculations, Journal of Raman Spectroscopy 43 (2012) 1065–1073. https://doi.org/10.1002/jrs.3127.

[86] L. Andernach, S. Pusch, C. Weber, D. Schollmeyer, S. Münster-Müller, M. Pütz, T. Opatz, Absolute configuration of the synthetic cannabinoid MDMB-CHMICA with its chemical characteristics in illegal products, Forensic Toxicol 34 (2016) 344–352. https://doi.org/10.1007/s11419-016-0321-1.

[87] D. Spálovská, T. Maříková, M. Kohout, F. Králík, M. Kuchař, V. Setnička, Methylone and pentylone: structural analysis of new psychoactive substances, Forensic Toxicol 37 (2019) 366–377. https://doi.org/10.1007/s11419-019-00468-z.

[88] L.S. Mariotto, C.H.P. Rodrigues, A.T. Bruni, Does Conformation Affect the Analytical Response? A Structural and Infrared Spectral Evaluation of Phenethylamines (2C-H, 25H-NBOH, and 25I-NBOMe) Using In Silico Methodology, Psychoactives 3 (2024) 78–92. https://doi.org/10.3390/psychoactives3010006.

[89] G. Peach, Theory of the pressure broadening and shift of spectral lines, Adv Phys 30 (1981) 367–474. https://doi.org/10.1080/00018738100101467.

[90] M.S. Bradley, C. Bratu, Vibrational Line Profiles as a Probe of Molecular Interactions, J Chem Educ 74 (1997) 553. https://doi.org/10.1021/ed074p553.

[91] G.H. Major, V. Fernandez, N. Fairley, M.R. Linford, A detailed view of the Gaussian–Lorentzian sum and product functions and their comparison with the Voigt function, Surface and Interface Analysis 54 (2022) 262–269. https://doi.org/10.1002/sia.7050.

[92] A. Carolina Sparavigna, Convolution and Fourier Transform: from Gaussian and Lorentzian Functions to q-Gaussian Tsallis Functions, Int J Sci 12 (2023) 7–11. https://doi.org/10.18483/ijSci.2732.

[93] V. Minaeva, B. Minaev, A. Panchenko, V. Pasychnik, Computational study of IR, Raman, and NMR spectra of 4-methylmethcathinone drug, J Mol Model 27 (2021) 3. https://doi.org/10.1007/s00894-020-04658-0.

[94] R. Öberg, L. Landström, E. Gracia-Espino, A. Larsson, M. Andersson, P.O. Andersson, Characterization of carfentanil and thiofentanil using surface-enhanced Raman spectroscopy and density functional theory, Journal of Raman Spectroscopy 55 (2024) 481–492. https://doi.org/10.1002/jrs.6643.

[95] K. He, Filter Feature Selection for Unsupervised Clustering of Designer Drugs Using DFT Simulated IR Spectra Data, ACS Omega 6 (2021) 32151–32165. https://doi.org/10.1021/acsomega.1c04945.

[96] C. dos Santos, A.T. Bruni, Evaluation of Density Functional Theory-Generated Data for Infrared Spectroscopy of Novel Psychoactive Substances Using Unsupervised Learning, Psychoactives 2024, Vol. 3, Pages 265-284 3 (2024) 265–284. https://doi.org/10.3390/PSYCHOACTIVES3020017.

[97] L.F.C. Sinhorini, C.H.P. Rodrigues, V.B.P. Leite, A.T. Bruni, Synthetic fentanyls evaluation and characterization by infrared spectroscopy employing in silico methods, Comput Theor Chem 1204 (2021) 113378. https://doi.org/10.1016/j.comptc.2021.113378.

[98] C. dos Santos, A.T. Bruni, Evaluation of Density Functional Theory-Generated Data for Infrared Spectroscopy of Novel Psychoactive Substances Using Unsupervised Learning, Psychoactives 3 (2024) 265–284. https://doi.org/10.3390/psychoactives3020017.

[99] T. Lu, F. Chen, Multiwfn: A multifunctional wavefunction analyzer, J Comput Chem 33 (2012) 580–592. https://doi.org/10.1002/jcc.22885.

[100] T. Bruhn, A. Schaumlöffel, Y. Hemberger, G. Bringmann, SpecDis: Quantifying the Comparison of Calculated and Experimental Electronic Circular Dichroism Spectra, Chirality 25 (2013) 243–249. https://doi.org/10.1002/chir.22138.

[101] L. Wang, C. Deriu, W. Wu, A.M. Mebel, B. McCord, Surface-enhanced Raman spectroscopy, Raman, and density functional theoretical analyses of fentanyl and six analogs, Journal of Raman Spectroscopy 50 (2019) 1405–1415. https://doi.org/10.1002/jrs.5656.

[102] M.A. Palafox, DFT computations on vibrational spectra: Scaling procedures to improve the wavenumbers, Physical Sciences Reviews 3 (2019). https://doi.org/10.1515/PSR-2017-0184/MACHINEREADABLECITATION/ENDNOTE.

[103] E.W. Ciurczak, B. Igne, J. Workman, D.A. Burns, Handbook of Near-Infrared Analysis, CRC Press, Fourth edition. | Boca Raton : Taylor and Francis, 2021. |, 2021. https://doi.org/10.1201/b22513.

[104] D.C. Young, Computational Chemistry, 1st ed., John Wiley & Sons, Inc., New York, USA, 2001. https://doi.org/10.1002/0471220655.

[105] J. Džodić, D. Milenković, M. Marković, Z. Marković, D. Dimić, Application of Quantum–Chemical Methods in the Forensic Prediction of Psychedelic Drugs' Spectra (IR, NMR, UV–VIS, and MS): A Case Study of LSD and Its Analogs, Applied Sciences 13 (2023) 2984. https://doi.org/10.3390/app13052984.

[106] L.P.L. Fávero, P.P. Belfiore, Manual de Análise de Dados - Estatística e Modelagem Multivariada com Excel®, SPSS® e Stata®, 1ª Edição, Elsevier, Rio de Janeiro, 2017.

[107] M. Prasath, S. Muthu, R. Arun Balaji, Vibrational spectroscopy investigation using ab initio and DFT vibrational analysis of 7-chloro-2-methylamino-5-phenyl-3H-1,4-benzodiazepine-4-oxide, Spectrochim Acta A Mol Biomol Spectrosc 113 (2013) 224–235. https://doi.org/10.1016/j.saa.2013.04.104.

[108] G. Baranović, Understanding the conformational, electronic and vibrational properties of Tetrahydrocannabinol (THC) and Cannabidiol (CBD). Pharmacophoric similarities and differences, J Mol Struct 1244 (2021) 130945. https://doi.org/10.1016/j.molstruc.2021.130945.

[109] M. Baranska, A. Kaczor, Morphine studied by vibrational spectroscopy and DFT calculations, Journal of Raman Spectroscopy 43 (2012) 102–107. https://doi.org/10.1002/jrs.3005.

[110] S. Sarala, S.K. Geetha, S. Muthu, A. Irfan, Computational investigation, comparative approaches, molecular structural, vibrational spectral, non-covalent interaction (NCI), and electron excitations analysis of benzodiazepine derivatives, J Mol Model 27 (2021) 266. https://doi.org/10.1007/s00894-021-04877-z.

[111] U. Holikulov, A.S. Kazachenko, N. Issaoui, A.S. Kazachenko, M. Raja, O.M. Al-Dossary, Z. Xiang, The molecular structure, vibrational spectra, solvation effect, non-covalent interactions investigations of psilocin, Spectrochim Acta A Mol Biomol Spectrosc 320 (2024) 124600. https://doi.org/10.1016/j.saa.2024.124600.

[112] G. Mahalakshmi, V. Balachandran, NBO, HOMO, LUMO analysis and vibrational spectra (FTIR and FT Raman) of 1-Amino 4-methylpiperazine using ab initio HF and DFT methods, Spectrochim Acta A Mol Biomol Spectrosc 135 (2015) 321–334. https://doi.org/10.1016/j.saa.2014.06.157.

[113] J. Mielcarek, D.M. Nowak, A. Pajzderska, B. Peplińska, J. Wąsicki, A hybrid method for estimation of molecular dynamics of diazepam-density functional theory combined with NMR and FT-IR spectroscopy, Int J Pharm 404 (2011) 19–26. https://doi.org/10.1016/j.ijpharm.2010.10.044.

[114] M.P. Dybowski, P. Holowinski, R. Typek, A.L. Dawidowicz, Comprehensive analytical and structural characteristics of methyl 3,3-dimethyl-2-(1-(pent-4-en-1-yl)-1H-indazole-3-carboxamido)butanoate (MDMB-4en-PINACA), Forensic Toxicol 39 (2021) 481–492. https://doi.org/10.1007/s11419-021-00573-y.

[115] K. Lopes, M. Lucena, T.I. Lopes, Á. da Silva, L. da Silva, N. Monteiro, P. de Lima-Neto, N. Ricardo, In silico and Experimental Assessments Applied to Preliminary Identification of New Illicit Substances Structures, J Braz Chem Soc (2024). https://doi.org/10.21577/0103-5053.20230090.

[116] A. Bhaskarapillai, S. Parayil, J. Santhamma, D. Mangalam, V.M.T. Anandakumar, Exploring the structural and electronic characteristics of phenethylamine derivatives: a density functional theory approach, Journal of Engineering and Applied Science 71 (2024) 136. https://doi.org/10.1186/s44147-024-00461-3.

[117] N. Öner, Ö. Tamer, D. Avcı, Y. Atalay, Conformational, spectroscopic and nonlinear optical properties of biologically active N,N-dimethyltryptamine molecule: A theoretical study, Spectrochim Acta A Mol Biomol Spectrosc 133 (2014) 542–549. https://doi.org/10.1016/j.saa.2014.06.037.

[118] H. Tavakol, M. Esfandyari, S. Taheri, A. Heydari, Investigation of structure, vibrational and NMR spectra of oxycodone and naltrexone: A combined experimental and theoretical study, Spectrochim Acta A Mol Biomol Spectrosc 79 (2011) 574–582. https://doi.org/10.1016/j.saa.2011.03.038.

[119] G.O. Ildiz, A.M. Tabanez, A. Nunes, J.P.L. Roque, L.L.G. Justino, M.L. Ramos, R. Fausto, Molecular structure, spectroscopy and photochemistry of alprazolam, J Mol Struct 1247 (2022) 131295. https://doi.org/10.1016/j.molstruc.2021.131295.

[120] K. Dobšíková, D. Spálovská, M. Kuchař, N. Paškanová, V. Setnička, Indazole-derived synthetic cannabinoids: Absolute configuration determination and structure characterization by circular

dichroism and DFT calculations, Spectrochim Acta A Mol Biomol Spectrosc 291 (2023) 122373. https://doi.org/10.1016/j.saa.2023.122373.

[121] S.K. Srivastava, V.B. Singh, Ab initio and DFT studies of the structure and vibrational spectra of anhydrous caffeine, Spectrochim Acta A Mol Biomol Spectrosc 115 (2013) 45–50. https://doi.org/10.1016/j.saa.2013.06.005.

[122] NIST Standard Reference Database 101, Computational Chemistry Comparison and Benchmark DataBase, Release 18, National Institute of Standards and Technology (2016).

[123] K.K. Irikura, R.D. Johnson, R.N. Kacker, Uncertainties in Scaling Factors for ab Initio Vibrational Frequencies, J Phys Chem A 109 (2005) 8430–8437. https://doi.org/10.1021/jp052793n.

[124] P. Fagan, D. Spálovská, R. Jurok, M. Kuchař, V. Schrenková, V. Setnička, Structural analysis of MDMA in solution by methods of chiroptical spectroscopy supported by DFT calculations, Vib Spectrosc 114 (2021) 103255. https://doi.org/10.1016/j.vibspec.2021.103255.

[125] S. Scientific Working Group on Drugs and Crime, SWGDRUG IR Spectral Library Version 3.1, SWGDRUG (2024). https://swgdrug.org/ir.htm (accessed November 15, 2024).

[126] European Network of Forensic Science Institutes Drug Working Group (ENFSIDWG)), ENFSI DWG IR Library: JCAMP-DX - 2024.08.05, ENFSI (2024). https://enfsi.eu/about-enfsi/structure/working-groups/drugs/ (accessed January 27, 2024).

[127] J.E. Nycz, G. Malecki, M. Zawiazalec, T. Pazdziorek, P. Skop, 1-Pentyl-3-(4-methoxy-1-naphthoyl)indole and 2-(2-methoxy-phenyl)-1-(1-pentyl-1H-indol-3-yl)-ethanone: X-ray structures and computational studies, J Mol Struct 984 (2010) 125–130. https://doi.org/10.1016/j.molstruc.2010.09.016.

[128] J.E. Nycz, G. Malecki, M. Zawiazalec, T. Pazdziorek, X-ray structures and computational studies of several cathinones, J Mol Struct 1002 (2011) 10–18. https://doi.org/10.1016/j.molstruc.2011.06.030.

[129] K. Nagarajan, N. Surumbarkuzhali, K. Parimala, Spectral analysis (FT-IR, FT-Raman, UV and NMR), molecular docking, ADMET properties and computational studies: 2-Hydroxy-5-nitrobenzaldehyde, Journal of the Indian Chemical Society 100 (2023) 100927. https://doi.org/10.1016/j.jics.2023.100927.

[130] C. Spearman, The Proof and Measurement of Association between Two Things, Am J Psychol 15 (1904) 72. https://doi.org/10.2307/1412159.

[131] K. Pearson, VII. Note on regression and inheritance in the case of two parents, Proceedings of the Royal Society of London 58 (1895) 240–242. https://doi.org/10.1098/rspl.1895.0041.

[132] H. Khamis, Measures of Association: How to Choose?, Journal of Diagnostic Medical Sonography 24 (2008) 155–162. https://doi.org/10.1177/8756479308317006.

[133] A. Singhal, Modern Information Retrieval: A Brief Overview, IEEE Computer Society Technical Committee on Data Engineering 4 (2001) 35–43. http://singhal.info/ieee2001.pdf (accessed November 3, 2024).

[134] P. Jaccard, THE DISTRIBUTION OF THE FLORA IN THE ALPINE ZONE, New Phytologist 11 (1912) 37–50. https://doi.org/10.1111/j.1469-8137.1912.tb05611.x.

[135] C.L. Covington, P.L. Polavarapu, CDSpecTech: A single software suite for multiple chiroptical spectroscopic analyses, Chirality 29 (2017) 178–192. https://doi.org/10.1002/chir.22691.

[136] Y.B. Monakhova, U. Holzgrabe, B.W.K. Diehl, Current role and future perspectives of multivariate (chemometric) methods in NMR spectroscopic analysis of pharmaceutical products, J Pharm Biomed Anal 147 (2018) 580–589. https://doi.org/10.1016/j.jpba.2017.05.034.

[137] R. Kumar, V. Sharma, Chemometrics in forensic science, TrAC Trends in Analytical Chemistry 105 (2018) 191–201. https://doi.org/10.1016/j.trac.2018.05.010.

[138] M.G. Md Ghazi, L.C. Lee, H. Sino, M.I. Abdul Halim, Review of contemporary chemometric strategies applied on preparing GC–MS data in forensic analysis, Microchemical Journal 181 (2022) 107732. https://doi.org/10.1016/j.microc.2022.107732.

[139] J. Miller, J.C. Miller, R.D. Miller, Statistics and Chemometrics for Analytical Chemistry, 7th ed., Pearson Education Limited, 2018.

[140] F. Zapata, F.E. Ortega-Ojeda, C. García-Ruiz, Forensic examination of textile fibres using Raman imaging and multivariate analysis, Spectrochim Acta A Mol Biomol Spectrosc 268 (2022) 120695. https://doi.org/10.1016/j.saa.2021.120695.

[141] M.C.A. Marcelo, K.C. Mariotti, R.S. Ortiz, M.F. Ferrão, M.J. Anzanello, Scott test evaluation by multivariate image analysis in cocaine samples, Microchemical Journal 127 (2016) 87–93. https://doi.org/10.1016/j.microc.2016.02.012.

[142] C. Cassino, C. Tsolakis, F. Bonello, V. Gianotti, D. Osella, Wine evolution during bottle aging, studied by 1H NMR spectroscopy and multivariate statistical analysis, Food Research International 116 (2019) 566–577. https://doi.org/10.1016/j.foodres.2018.08.075.

[143] B.G. Tabachnick, L.S. Fidell, Using Multivariate Statistics, Sixth Edition, Pearson, 2012.

[144] Y. Tominaga, Comparative study of class data analysis with PCA-LDA, SIMCA, PLS, ANNs, and k-NN, Chemometrics and Intelligent Laboratory Systems 49 (1999) 105–115. https://doi.org/10.1016/S0169-7439(99)00034-9.

[145] M.M.C. Ferreira, QUIMIOMETRIA - Conceitos, Métodos e Aplicações, 1st ed., Editora da Unicamp, Campinas, 2015.

[146] K.R. Padma, K.R. Don, Artificial Neural Network Applications in Analysis of Forensic Science, in: Cyber Security and Digital Forensics, Wiley, 2022: pp. 59–72. https://doi.org/10.1002/9781119795667.ch3.

[147] T. Fawcett, An introduction to ROC analysis, Pattern Recognit Lett 27 (2006) 861–874. https://doi.org/10.1016/j.patrec.2005.10.010.

[148] D. Chicco, G. Jurman, The advantages of the Matthews correlation coefficient (MCC) over F1 score and accuracy in binary classification evaluation, BMC Genomics 21 (2020) 6. https://doi.org/10.1186/s12864-019-6413-7.

[149] B.W. Matthews, Comparison of the predicted and observed secondary structure of T4 phage lysozyme, Biochimica et Biophysica Acta (BBA) - Protein Structure 405 (1975) 442–451. https://doi.org/10.1016/0005-2795(75)90109-9.

[150] D.M.W. Powers, Evaluation: from precision, recall and F-measure to ROC, informedness, markedness and correlation, International Journal of Machine Learning Technology 2 (2011) 37–63. http://arxiv.org/abs/2010.16061.

[151] A.M. Sila, K.D. Shepherd, G.P. Pokhariyal, Evaluating the utility of mid-infrared spectral subspaces for predicting soil properties, Chemometrics and Intelligent Laboratory Systems 153 (2016). https://doi.org/10.1016/j.chemolab.2016.02.013.

[152] S.F. Williams, R. Stokes, P.L. Tang, A.M. Blanco-Rodriguez, Detection & identification of hazardous narcotics and new psychoactive substances using Fourier transform infrared spectroscopy (FTIR), Analytical Methods 15 (2023) 3225–3232. https://doi.org/10.1039/d3ay00766a.

[153] Q.T. Whiting, K.F. O'Connor, P.M. Potter, S.R. Al-Abed, A high-throughput, automated technique for microplastics detection, quantification, and characterization in surface waters using laser direct infrared spectroscopy, Anal Bioanal Chem 414 (2022). https://doi.org/10.1007/s00216-022-04371-2.

[154] ThermoFisherInc., Analytical Methods for Field-Based Material Identification and Verification, (2014). http://tools.thermofisher.com/content/sfs/brochures/TS-Pharma-pvalue-HQI.pdf.

[155] B.K. Lavine, C.G. White, M.D. Allen, A. Weakley, Pattern recognition-assisted infrared library searching of the paint data query database to enhance lead information from automotive paint trace evidence, Appl Spectrosc 71 (2017) 480–495. https://doi.org/10.1177/0003702816666287.

[156] K.R. Palomino Pacheco, C.R. Berdugo Correa, Statistical analysis and machine learning in psychoactive substance use: a bibliometric analysis, Nexo Revista Científica 36 (2023) 96–109. https://doi.org/10.5377/nexo.v36i02.16017.

[157] A.A. Bunaciu, H.Y. Aboul-Enein, Adulterated drug analysis using FTIR spectroscopy, Appl Spectrosc Rev 56 (2021) 423–437. https://doi.org/10.1080/05704928.2020.1811717.

[158] C.K. Muro, K.C. Doty, J. Bueno, L. Halámková, I.K. Lednev, Forensic Applications of Vibrational Spectroscopy, in: Forensic Sci, Wiley-VCH Verlag GmbH & Co. KGaA, Weinheim, Germany, 2016: pp. 5–54. https://doi.org/10.1002/9783527693535.ch2.

[159] A. Takamura, T. Ozawa, Recent advances of vibrational spectroscopy and chemometrics for forensic biological analysis, Analyst 146 (2021) 7431–7449. https://doi.org/10.1039/D1AN01637G.

[160] A. Shafi, A.J. Berry, H. Sumnall, D.M. Wood, D.K. Tracy, New psychoactive substances: a review and updates, Ther Adv Psychopharmacol 10 (2020) 204512532096719. https://doi.org/10.1177/2045125320967197.

[161] M. Evans-Brown, R. Sedefov, New psychoactive substances: driving greater complexity into the drug problem, Addiction 112 (2017) 36–38. https://doi.org/10.1111/add.13528.

[162] R. Solimini, M.C. Rotolo, M. Pellegrini, A. Minutillo, R. Pacifici, F.P. Busardò, S. Zaami, Adulteration Practices of Psychoactive Illicit Drugs: An Updated Review, Curr Pharm Biotechnol 18 (2017). https://doi.org/10.2174/1389201018666170710184531.

[163] R.F. Kranenburg, H. Ramaker, S. Sap, A.C. van Asten, A calibration friendly approach to identify drugs of abuse mixtures with a portable near-infrared analyzer, Drug Test Anal 14 (2022) 1089–1101. https://doi.org/10.1002/dta.3231.

[164] S.A. Al, A.-R. Allouche, Neural Network Approach for Predicting Infrared Spectra from 3D Molecular Structure, Chemical Physics (Physics.Chem-Ph) (2024). https://doi.org/10.1016/j.cplett.2024.141603.

[165] Wiley Science Solutions, KnowItAll IR Spectral Database Collection, Wiley (2024).

[166] N. Saquer, R. Iqbal, J.D. Ellis, K. Yoshimatsu, Infrared spectra prediction using attention-based graph neural networks, Digital Discovery 3 (2024). https://doi.org/10.1039/d3dd00254c.

[167] B. Kirchweger, J.M. Rollinger, A Strength-Weaknesses-Opportunities-Threats (SWOT) Analysis of Cheminformatics in Natural Product Research, in: A. Kinghorn, H. Falk, S. Gibbons, J. Kobayashi, Y. Asakawa, J.K. Liu (Eds.), Prog Chem Org Nat Prod, Springer, Cham, 2019: pp. 239–271. https://doi.org/10.1007/978-3-030-14632-0_7.

[168] S. Huhtala, A. Nordgaard, B. Ahrens, I. Alberink, T. Korpinsalo, M. Bovens, Chemometrics in Forensic Chemistry – Part III: Quality assessment and interpretation of chemometric output, Forensic Sci Int 348 (2023) 111612. https://doi.org/10.1016/j.forsciint.2023.111612.

[169] P.A. Shinde, Q. Abbas, N.R. Chodankar, K. Ariga, M.A. Abdelkareem, A.G. Olabi, Strengths, weaknesses, opportunities, and threats (SWOT) analysis of supercapacitors: A review, Journal of Energy Chemistry 79 (2023) 611–638. https://doi.org/10.1016/j.jechem.2022.12.030.

[170] J. Pernaa, Possibilities and Challenges of Using Educational Cheminformatics for STEM Education: A SWOT Analysis of a Molecular Visualization Engineering Project, J Chem Educ 99 (2022) 1190–1200. https://doi.org/10.1021/acs.jchemed.1c00683.

[171] M.G. Miller, Environmental Metabolomics: A SWOT Analysis (Strengths, Weaknesses, Opportunities, and Threats), J Proteome Res 6 (2007) 540–545. https://doi.org/10.1021/pr060623x.